Metadynamics as a Post-Processing Method for Virtual Screening with Application to the Pseudokinase Domain of JAK2

Supporting Information

*Kara J. Cutrona, Ana S. Newton, Stefan G. Krimmer, Julian Tirado-Rives, and William L. Jorgensen**

Department of Chemistry, Yale University, New Haven, Connecticut 06520-8107

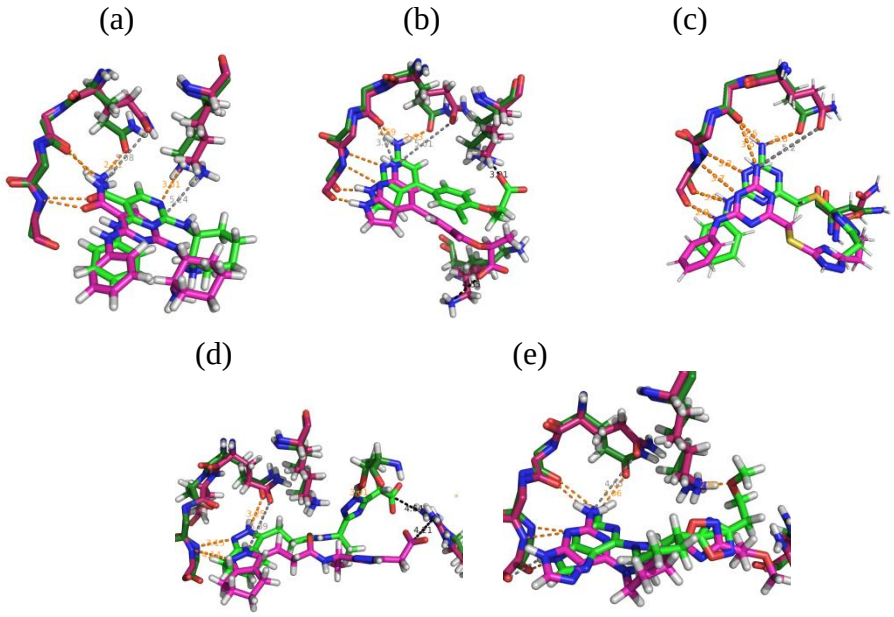

Figure S1. Green and pink structures show the changes before and after equilibration, respectively, for the following compounds: (a) PRT-6207629, (b) JAK-206, (c) JAK-207, (d) JAK-223 and (e) JAK-226.

PMF Curves of Benchmark Ligands (Crystal Structure Poses)

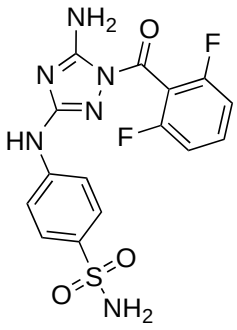

WC1 (K_d=0.456 μM)

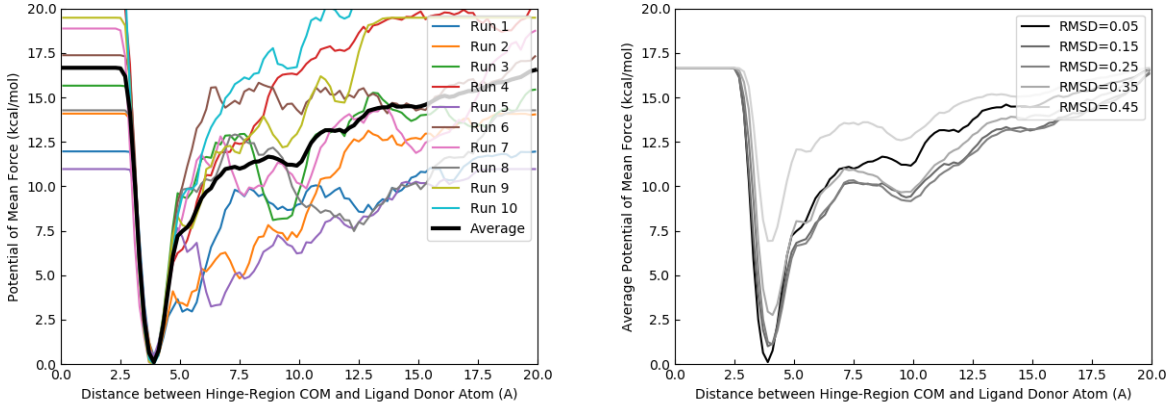

Figure S2.1. (a) WC1 structure (b) PMF curve of JH2/WC1 unbinding at 0.05 Å Val629 backbone RMSD (c) PMF curves of JH2/WC1 unbinding at highly-sampled Val629 backbone RMSDs. All PMF curves converged from 0 until at least 10 angstroms.

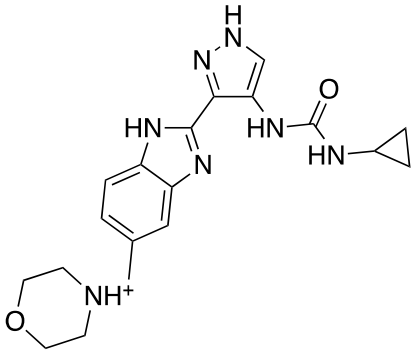

WC2 (K_d=19.5 μM)

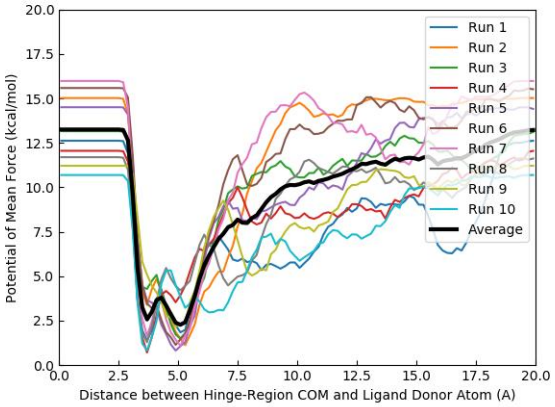

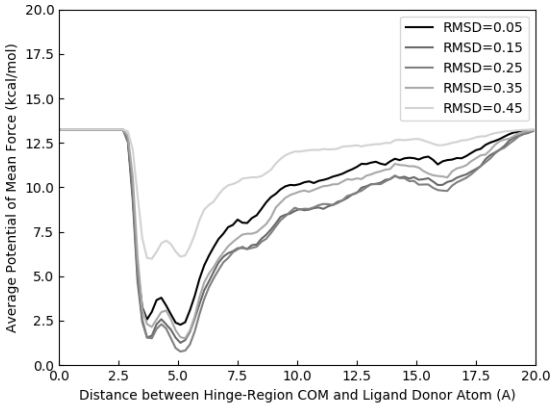

Figure S2.2. (a) WC2 structure (b) PMF curve of JH2/WC2 unbinding at 0.05 Å Val629 backbone RMSD (c) PMF curves of JH2/WC2 unbinding at highly-sampled Val629 backbone RMSDs. All PMF curves converged from 0 until at least 10 angstroms.

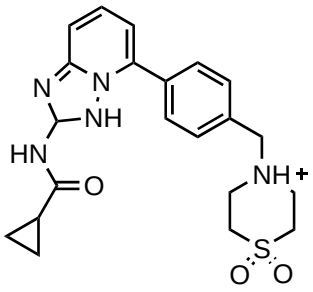

Filgotinib (Low activity, 9% at 50 μM)

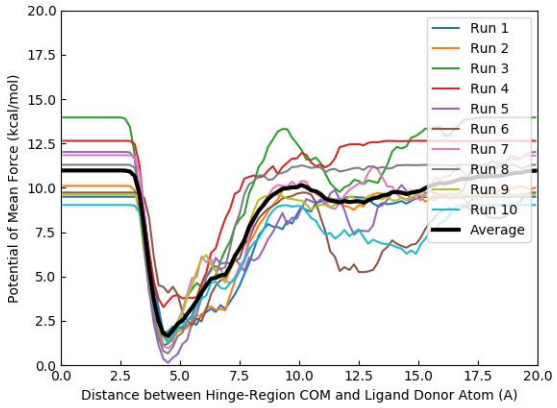

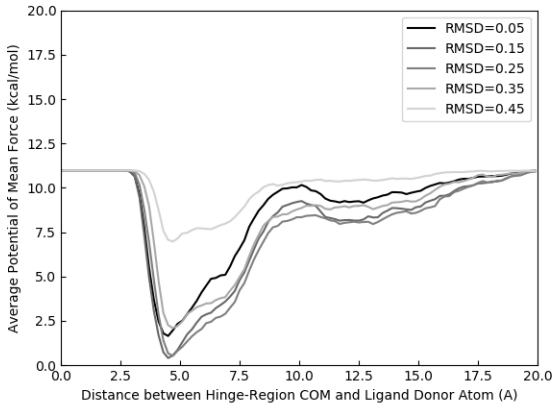

Figure S2.3. (a) Filgotinib structure (b) PMF curve of JH2/Filgotinib unbinding at 0.05 Å Val629 backbone RMSD (c) PMF curves of JH2/Filgotinib unbinding at highly-sampled Val629 backbone RMSDs. All PMF curves converged from 0 until at least 10 angstroms.

PMF Curves of Additional High Throughput Screen Ligands

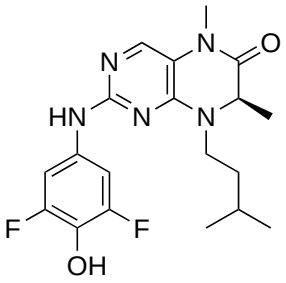

BI-D1870 (R)

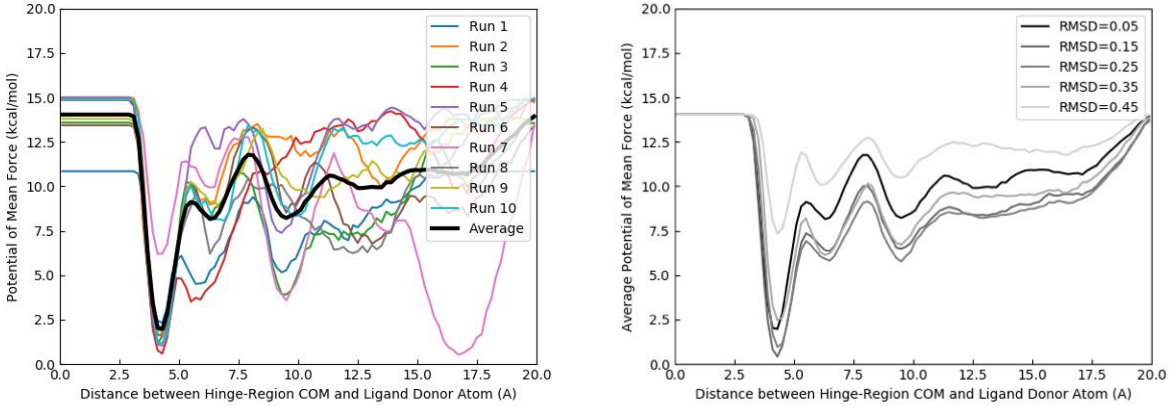

Figure S3.1. (a) BI-D1870(R) structure (b) PMF curve of JH2/BI-D1870(R) unbinding at 0.05 Å Val629 backbone RMSD (c) PMF curves of JH2/BI-D1870(R) unbinding at highly-sampled Val629 backbone RMSDs. All PMF curves converged from 0 until at least 10 angstroms.

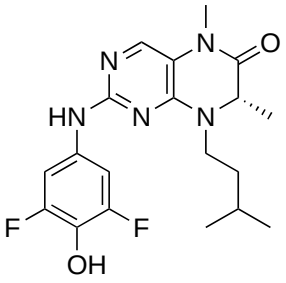

BI-D1870 (S)

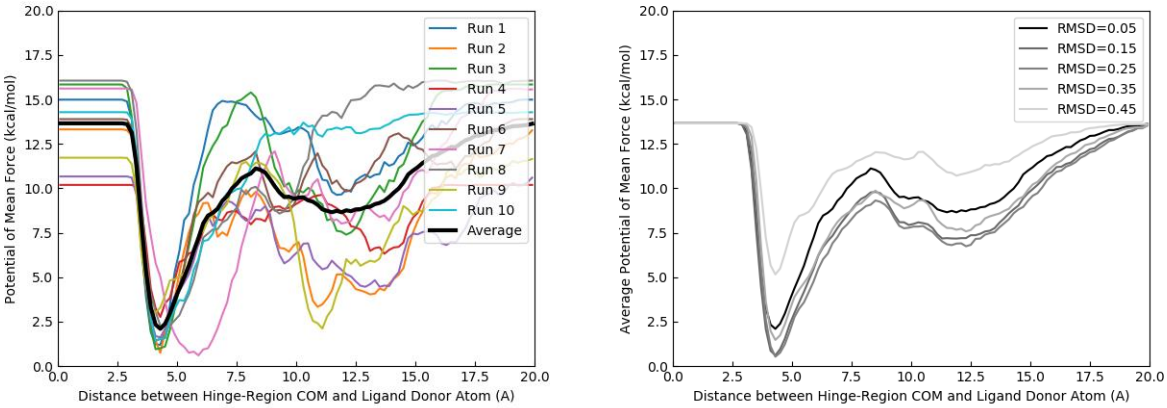

Figure S3.2. (a) BI-D1870(S) structure (b) PMF curve of JH2/BI-D1870(S) unbinding at 0.05 Å Val629 backbone RMSD (c) PMF curves of JH2/BI-D1870(S) unbinding at highly-sampled Val629 backbone RMSDs. All PMF curves converged from 0 until at least 10 angstroms.

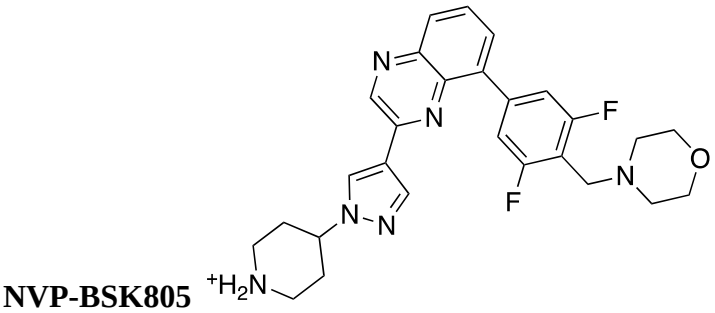

NVP-BSK805

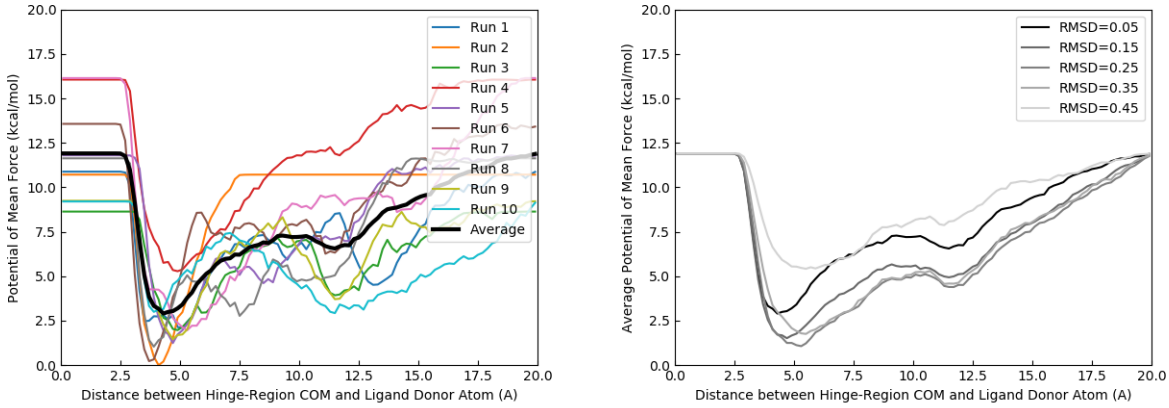

Figure S3.3. (a) NVP-BSK805 structure (b) PMF curve of JH2/NVP-BSK805 unbinding at 0.05 Å Val629 backbone RMSD (c) PMF curves of JH2/NVP-BSK805 unbinding at highly-sampled Val629 backbone RMSDs. All PMF curves converged from 0 until at least 10 angstroms. Run 2 was excluded in the PMF curve average because there was not enough sampling at 0.05 Å Val629 backbone RMSD.

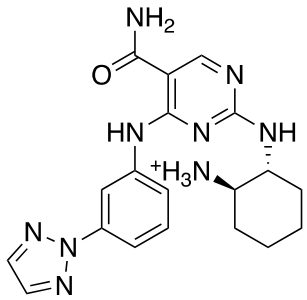

PRT062607

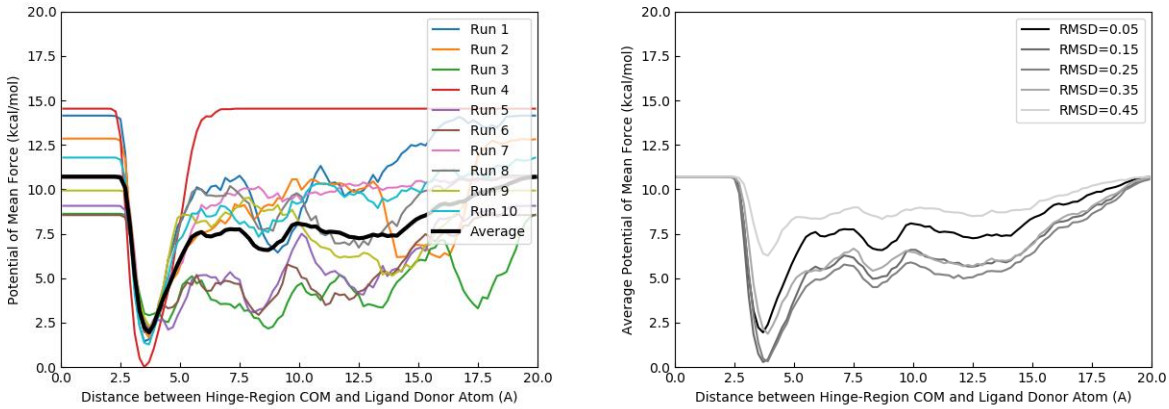

Figure S3.4. (a) PRT062607 structure (b) PMF curve of JH2/PRT062607 unbinding at 0.05 Å Val629 backbone RMSD (c) PMF curves of JH2/PRT062607 unbinding at highly-sampled Val629 backbone RMSDs. All PMF curves converged from 0 until at least 10 angstroms. Run 4 was excluded in the PMF curve average because there was not enough sampling at 0.05 Å Val629 backbone RMSD.

PMF Curves of Jorgensen Lab-Developed JAK2 JH2 Ligands

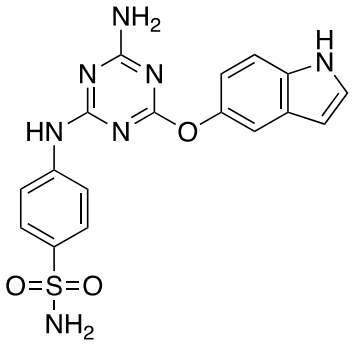

JAK-67

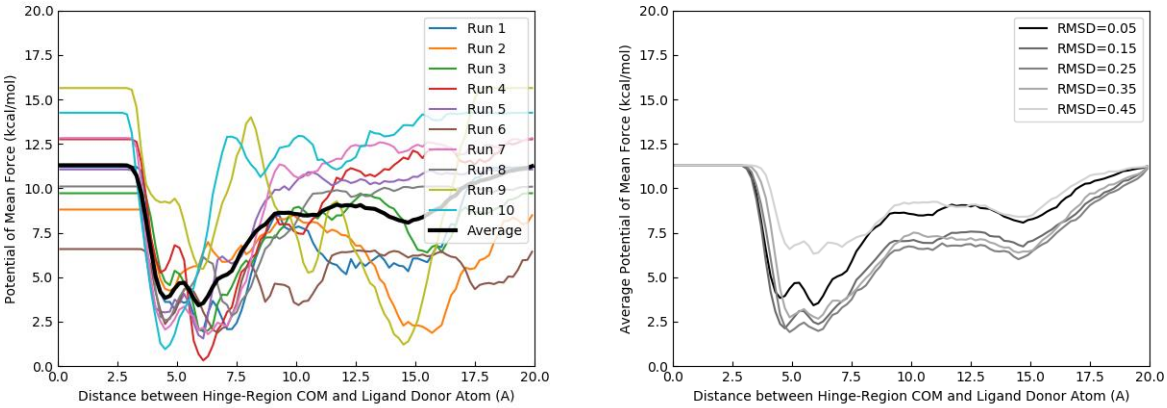

Figure S4.1. (a) JAK-67 structure (b) PMF curve of JH2/JAK-67 unbinding at 0.05 Å Val629 backbone RMSD (c) PMF curves of JH2/JAK-67 unbinding at highly-sampled Val629 backbone RMSDs. All PMF curves converged from 0 until at least 10 angstroms.

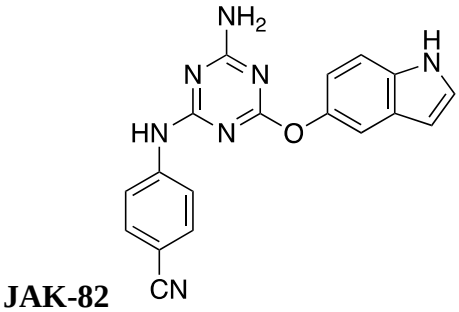

JAK-82

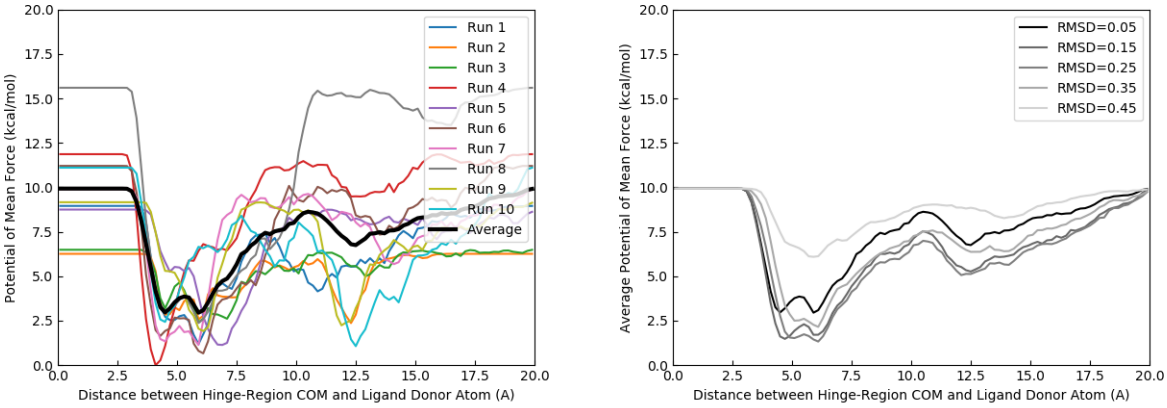

Figure S4.2. (a) JAK-82 structure (b) PMF curve of JH2-JAK82 unbinding at 0.05 Å Val629 backbone RMSD (c) PMF curves of JH2-JAK82 unbinding at highly-sampled Val629 backbone RMSDs. All PMF curves converged from 0 until at least 10 angstroms.

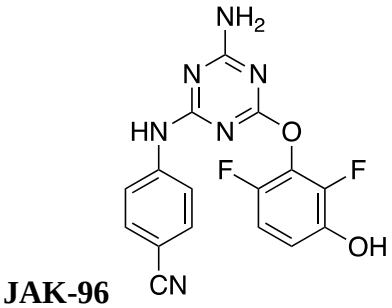

JAK-96

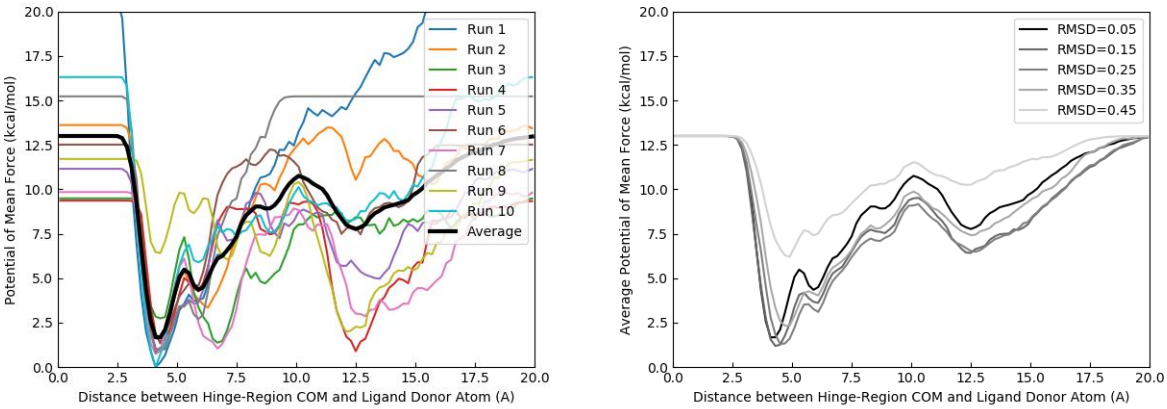

Figure S4.3. (a) JAK-96 structure (b) PMF curve of JH2-JAK96 unbinding at 0.05 Å Val629 backbone RMSD (c) PMF curves of JH2-JAK96 unbinding at highly-sampled Val629 backbone RMSDs. All PMF curves converged from 0 until at least 10 angstroms.

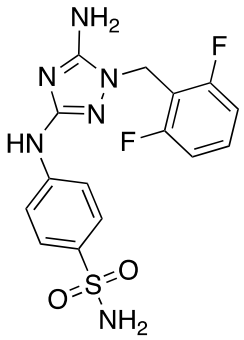

JAK-118

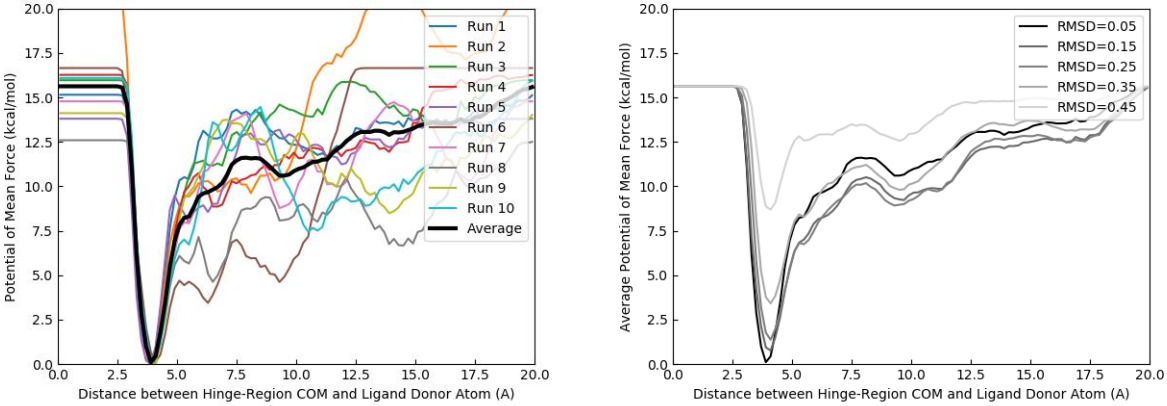

Figure S4.4. (a) JAK-118 structure (b) PMF curve of JH2/JAK-118 unbinding at 0.05 Å Val629 backbone RMSD (c) PMF curves of JH2/JAK-118 unbinding at highly-sampled Val629 backbone RMSDs. All PMF curves converged from 0 until at least 10 angstroms.

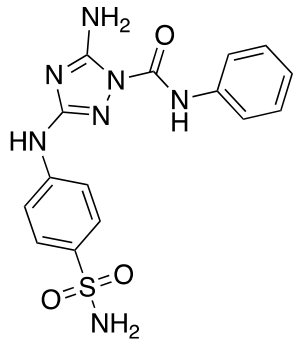

JAK-170

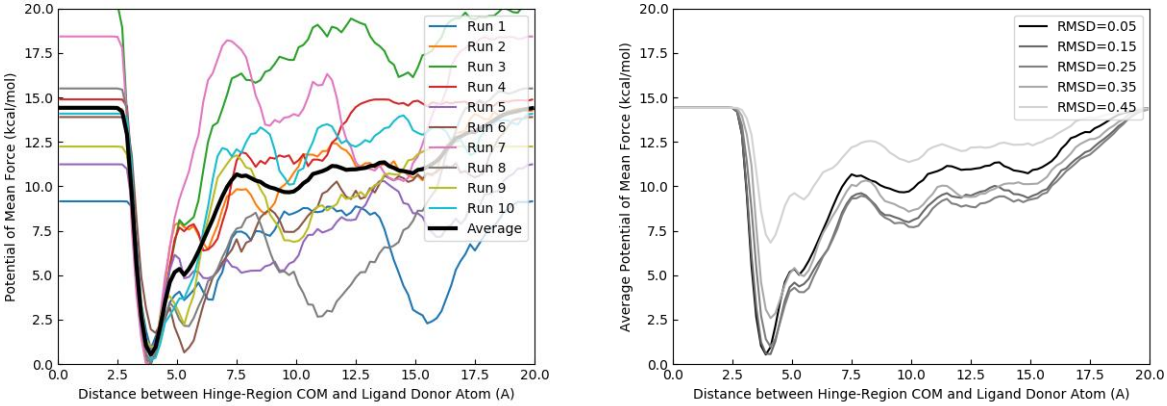

Figure S4.5. (a) JAK-170 structure (b) PMF curve of JH2/JAK-170 unbinding at 0.05 Å Val629 backbone RMSD (c) PMF curves of JH2/JAK-170 unbinding at highly-sampled Val629 backbone RMSDs. All PMF curves converged from 0 until at least 10 angstroms.

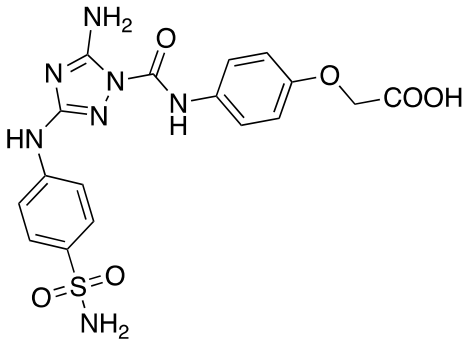

JAK-179

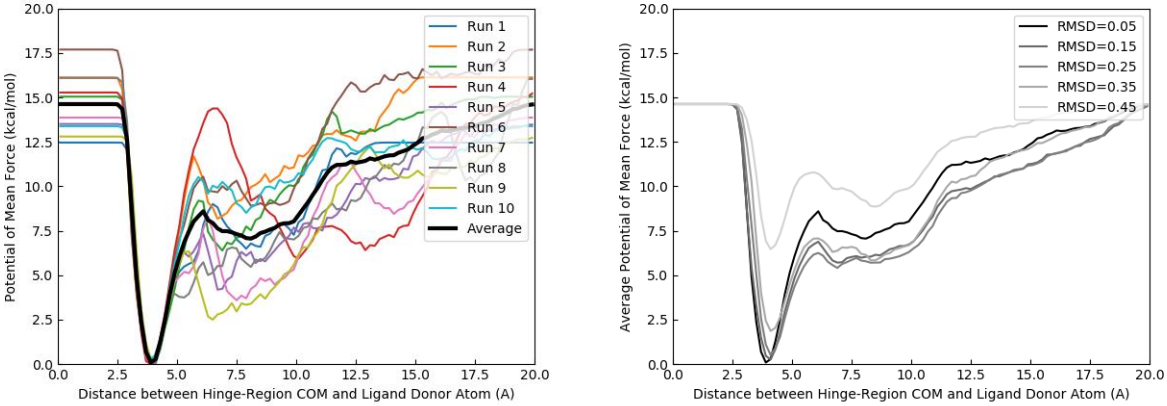

Figure S4.6. (a) JAK-179 structure (b) PMF curve of JH2/JAK-179 unbinding at 0.05 Å Val629 backbone RMSD (c) PMF curves of JH2-JAK179 unbinding at highly-sampled Val629 backbone RMSDs. All PMF curves converged from 0 until at least 10 angstroms.

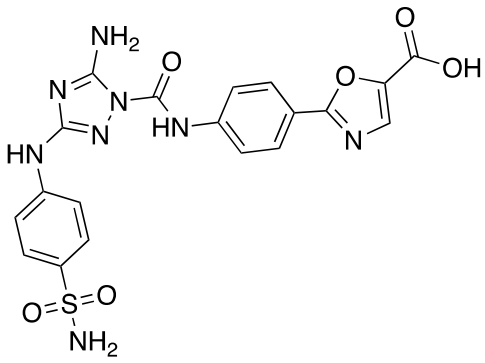

JAK-190

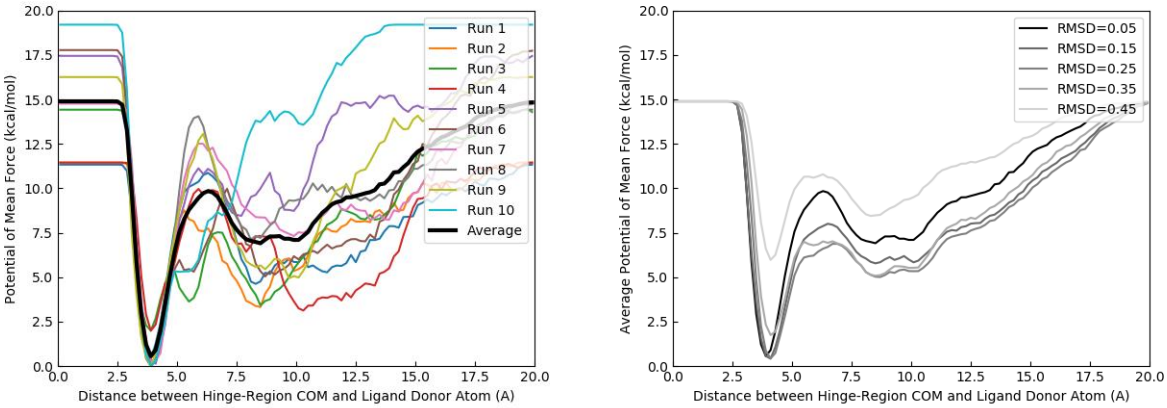

Figure S4.7. (a) JAK-190 structure (b) PMF curve of JH2-JAK190 unbinding at 0.05 Å Val629 backbone RMSD (c) PMF curves of JH2-JAK190 unbinding at highly-sampled Val629 backbone RMSDs. All PMF curves converged from 0 until at least 10 angstroms.

PMF Curves of Crystal Structure (CS) Poses versus Higher SP-scoring Non-CS Poses

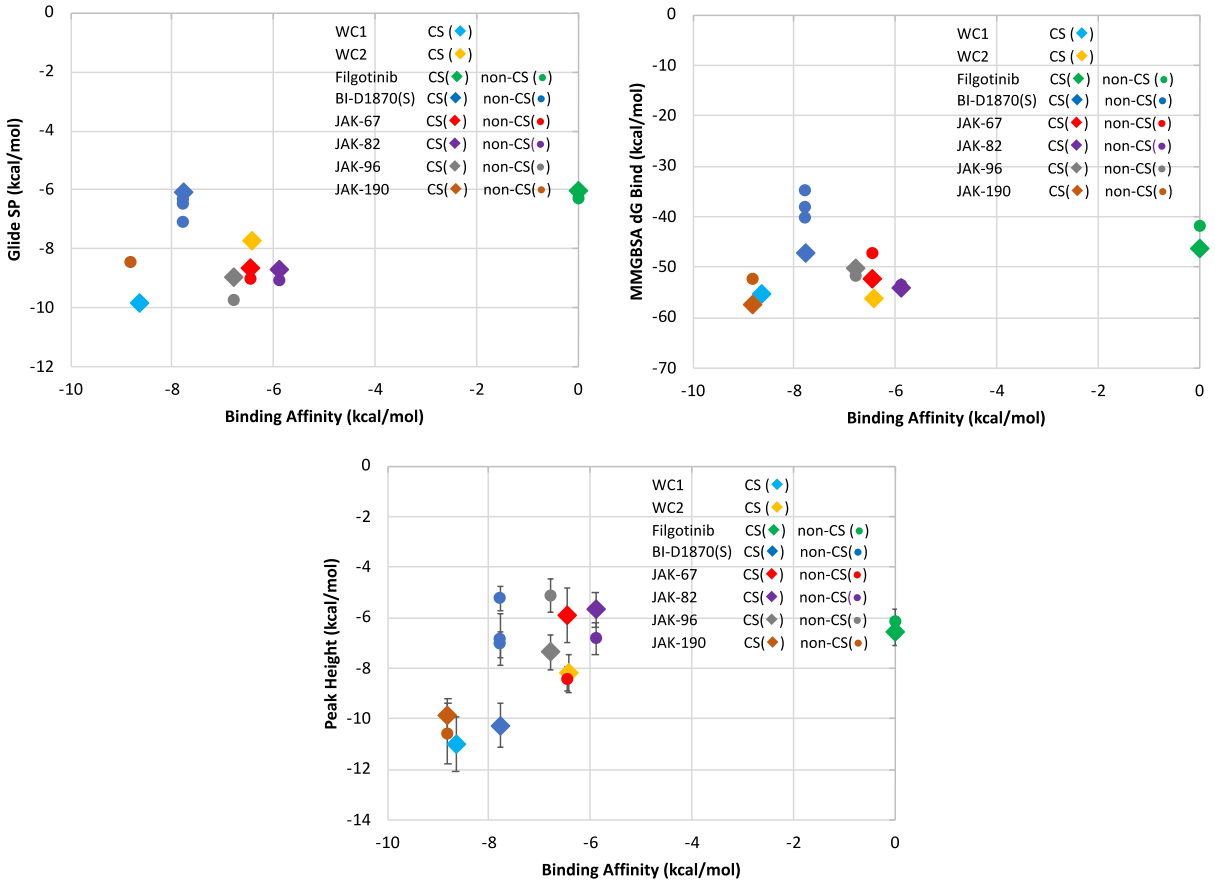

Figure S5.1. Comparison of the binding affinity of the ligand to the (a) Glide SP score, (b) MM/GBSA dG Bind and (c) peak height of the crystal structure and higher-ranked poses.

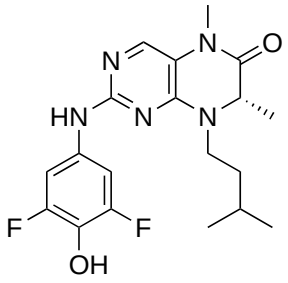

BI-D1870 (S)

Top Glide SP pose

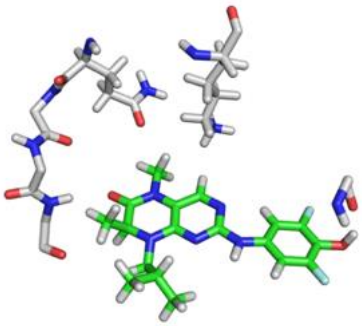

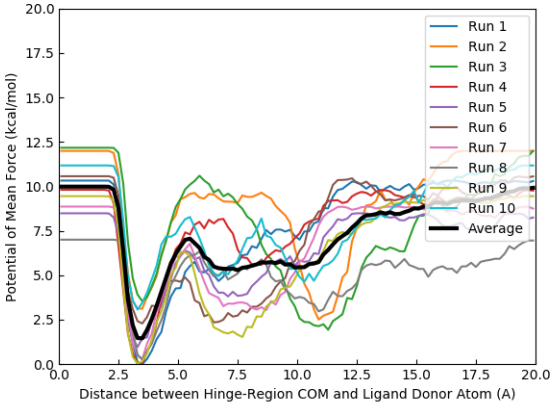

Second Glide SP pose

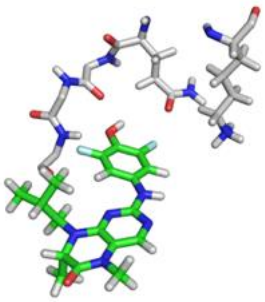

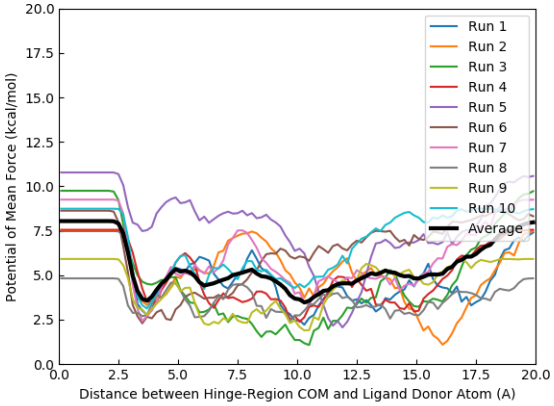

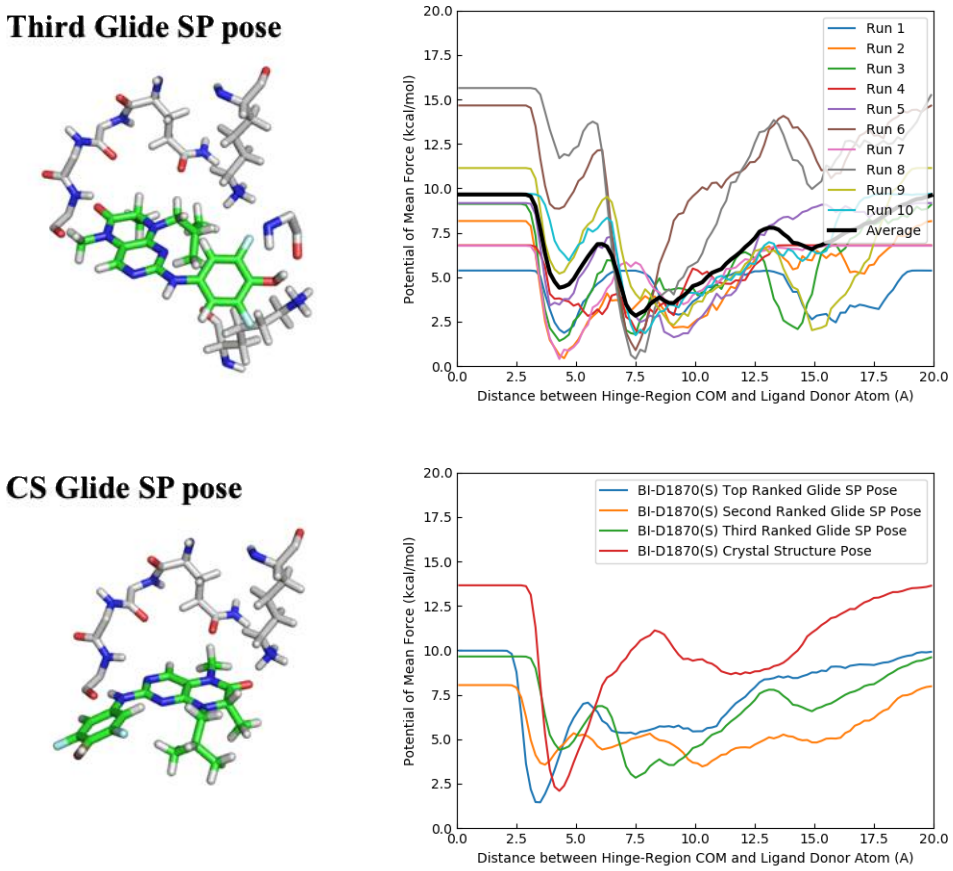

Figure S5.2. (a) BI-D1870(S) structure (b-d) For each higher-ranking Glide SP pose, [(I) JH2/BI-D1870(S) Glide SP pose (II) PMF curve of JH2-BI-D1870(S) unbinding at 0.05 Å Val629 backbone RMSD]. (e) BI-D1870(S) crystal structure pose (f) Comparison of average PMF curves of crystal structure pose and higher-ranking Glide SP poses for BI-D1870(S). All PMF curves converged from 0 until at least 10 angstroms.

Filgotinib

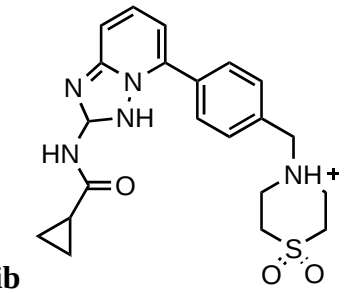

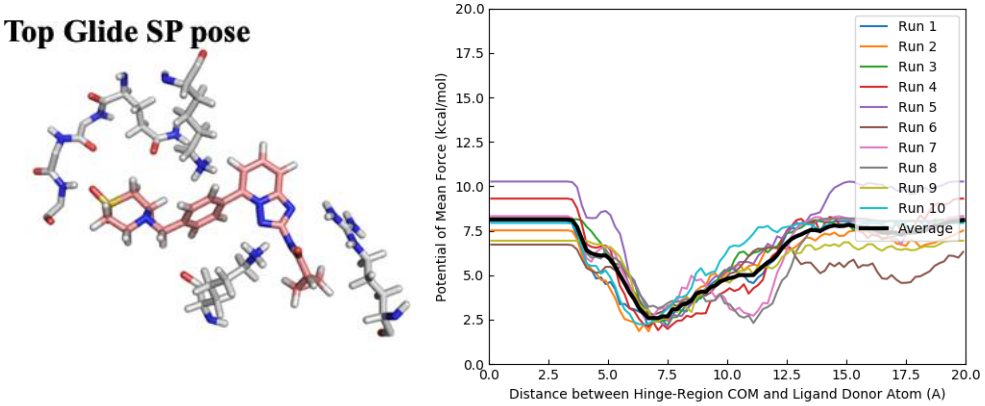

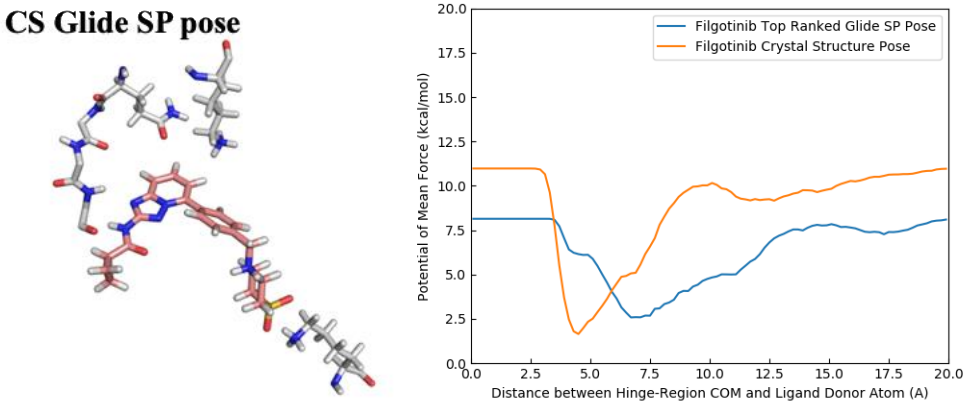

Figure S5.3. (a) Filgotinib structure (b) JH2/Filgotinib top Glide SP pose (c) PMF curve of JH2/Filgotinib (top pose) unbinding at 0.05 Å Val629 backbone RMSD (d) JH2/Filgotinib crystal structure pose (e) Comparison of average PMF curves of crystal structure pose and top Glide SP pose for Filgotinib. All PMF curves converged from 0 until at least 10 angstroms.

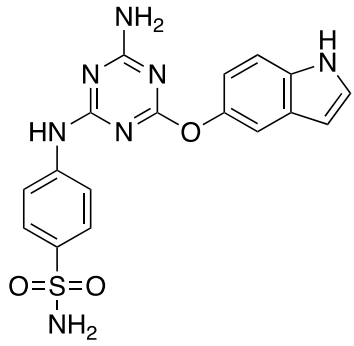

JAK-67

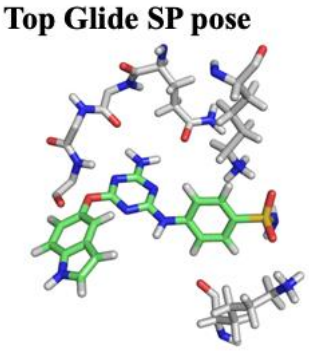

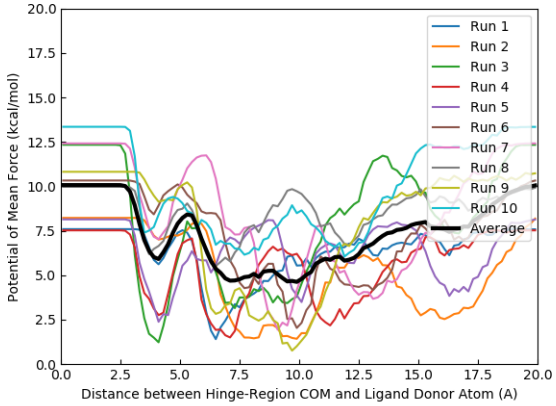

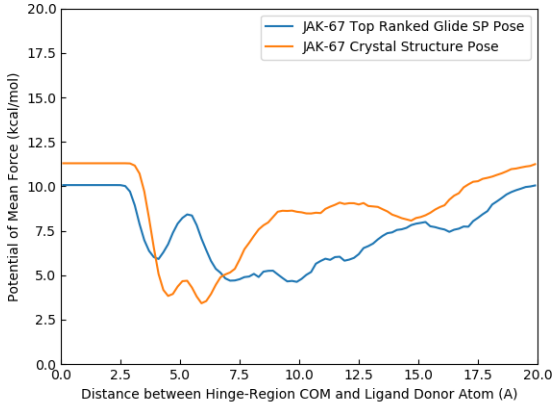

Figure S5.4. (a) JAK-67 structure (b) JH2/JAK-67 top Glide SP pose (c) PMF curve of JH2/JAK-67 (top pose) unbinding at 0.05 Å Val629 backbone RMSD (d) JH2/JAK-67 crystal structure pose (e) Comparison of average PMF curves of crystal structure pose and top Glide SP pose for JAK-67. All PMF curves converged from 0 until at least 10 angstroms.

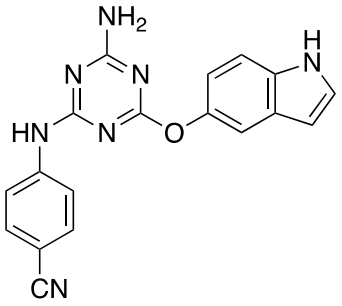

JAK-82

Top Glide SP pose

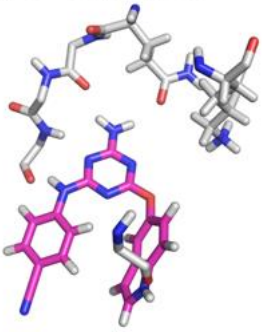

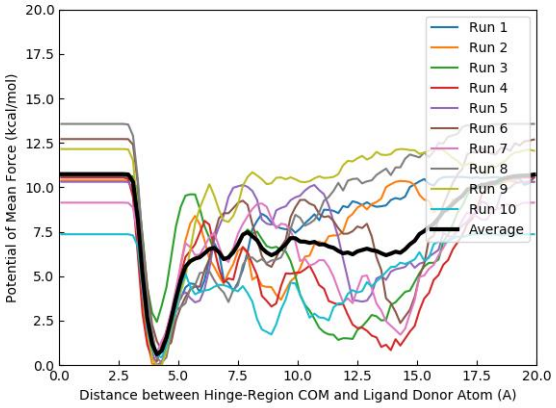

CS Glide SP pose

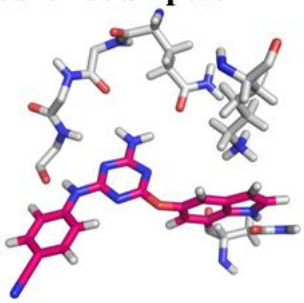

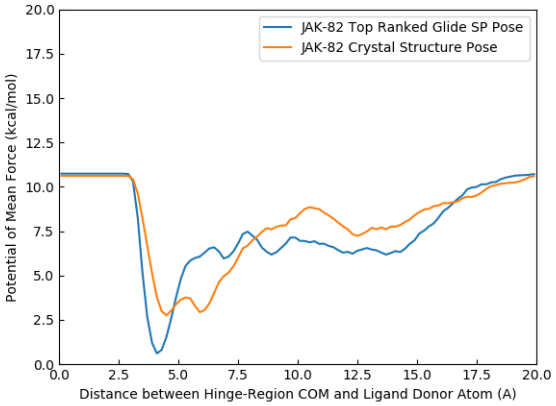

Figure S5.5. (a) JAK-82 structure (b) JH2/JAK-82 top Glide SP pose (c) PMF curve of JH2/JAK-82 (top pose) unbinding at 0.05 Å Val629 backbone RMSD (d) JH2/JAK-82 crystal structure pose based on JH2/JAK-67 crystal structure (e) Comparison of average PMF curves of crystal structure pose and top Glide SP pose for JAK-82. All PMF curves converged from 0 until at least 10 angstroms.

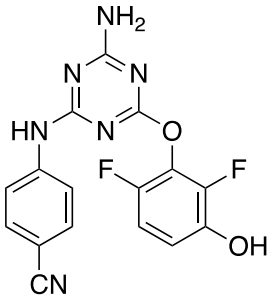

JAK-96

Top Glide SP pose

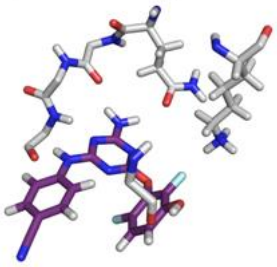

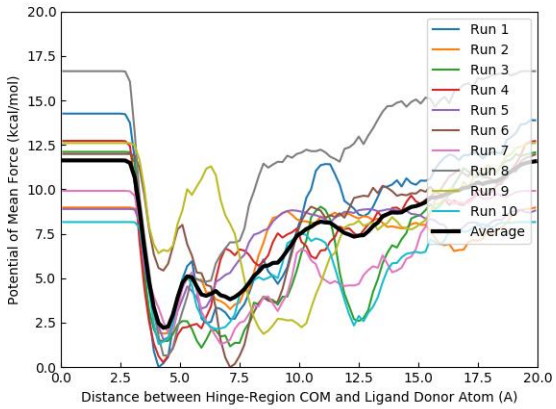

CS Glide SP pose

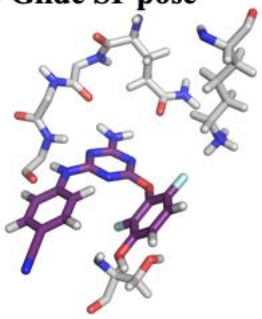

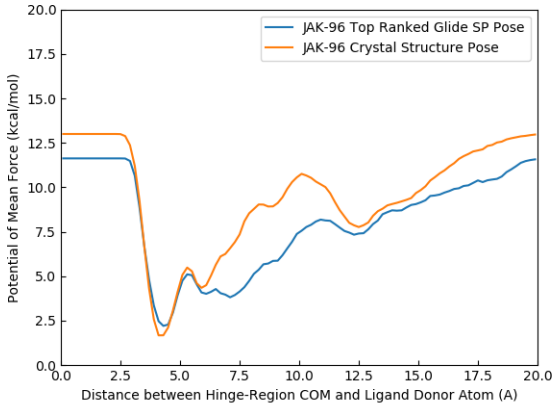

Figure S5.6. (a) JAK-96 structure (b) JH2/JAK-96 top Glide SP pose (c) PMF curve of JH2/JAK-96 (top pose) unbinding at 0.05 Å Val629 backbone RMSD (d) JH2/JAK-96 crystal structure pose (e) Comparison of average PMF curves of crystal structure pose and top Glide SP pose for JAK-96. All PMF curves converged from 0 until at least 10 angstroms.

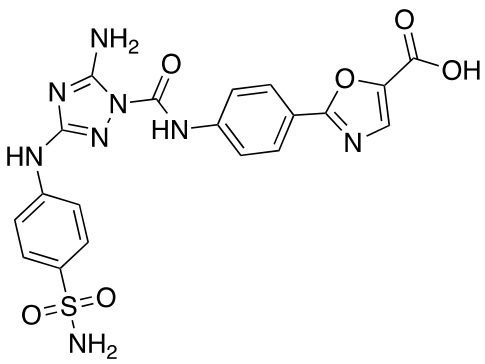

JAK-190

Top Glide SP pose

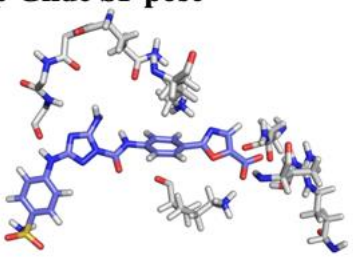

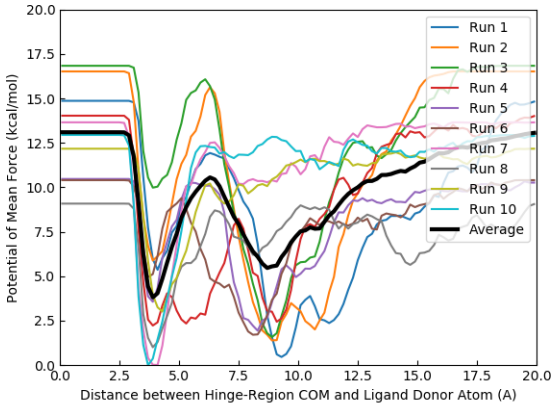

CS Glide SP pose

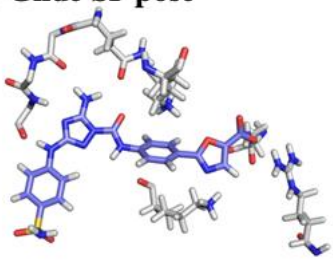

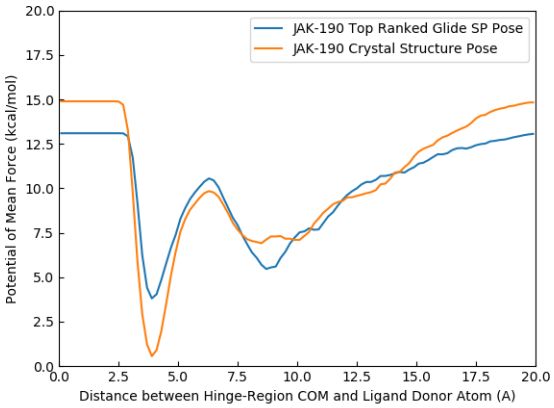

Figure S5.7. (a) JAK-190 structure (b) JH2/JAK-190 top Glide SP pose (c) PMF curve of JH2/JAK-190 (top pose) unbinding at 0.05 Å Val629 backbone RMSD (d) JH2/JAK-190 crystal structure pose (e) Comparison of average PMF curves of crystal structure pose and top Glide SP pose for JAK-190. All PMF curves converged from 0 until at least 10 angstroms.

PMF Curves of Virtual Screening Ligands

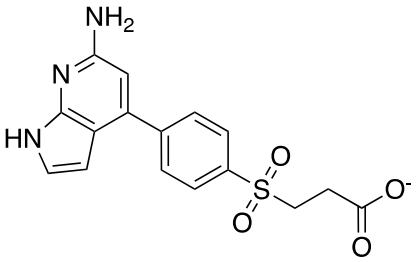

JAK-198

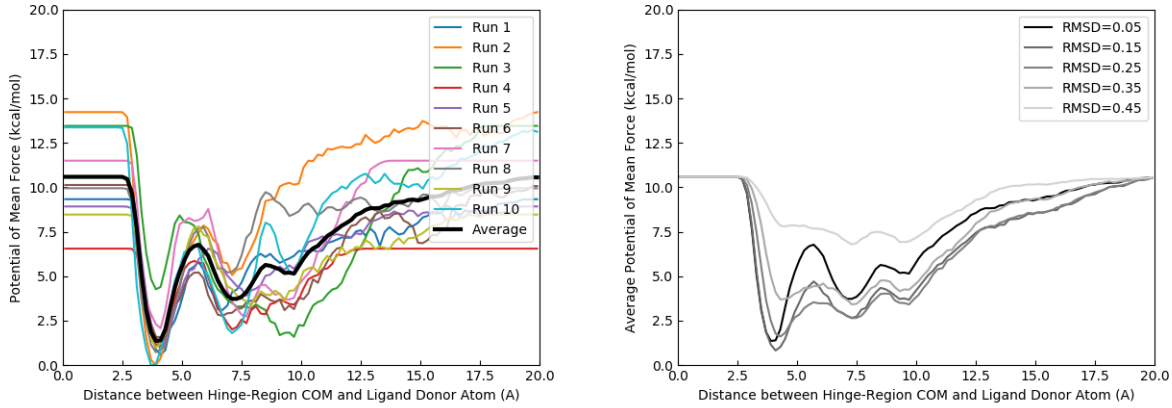

Figure S6.1. (a) JAK-198 structure (b) PMF curve of JH2/JAK-198 unbinding at 0.05 Å Val629 backbone RMSD (c) PMF curves of JH2/JAK-198 unbinding at highly-sampled Val629 backbone RMSDs. All PMF curves converged from 0 until at least 10 angstroms.

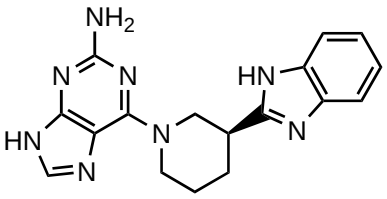

JAK-199

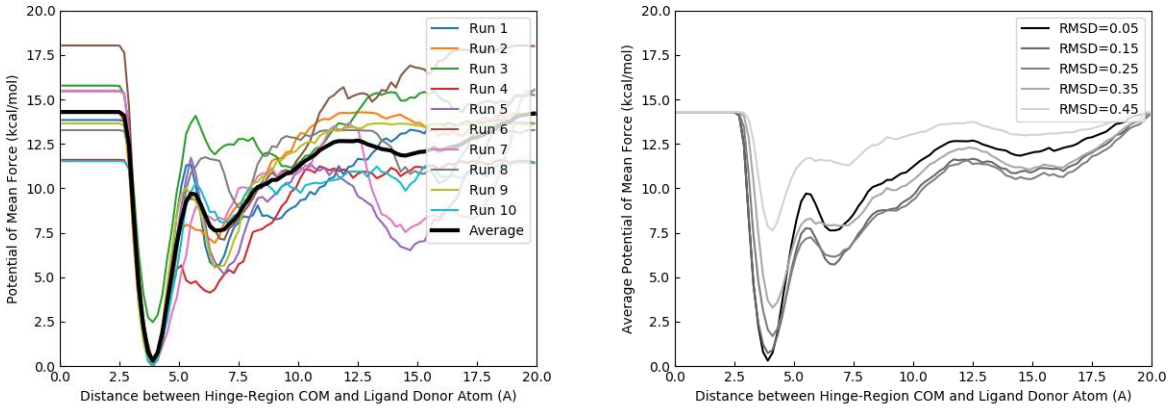

Figure S6.2. (a) JAK-199 structure (b) PMF curve of JH2/JAK-199 unbinding at 0.05 Å Val629 backbone RMSD (c) PMF curves of JH2/JAK-199 unbinding at highly-sampled Val629 backbone RMSDs. All PMF curves converged from 0 until at least 10 angstroms.

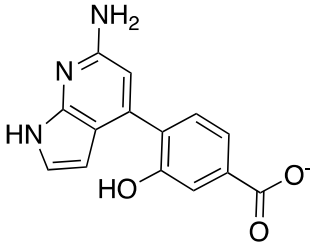

JAK-200

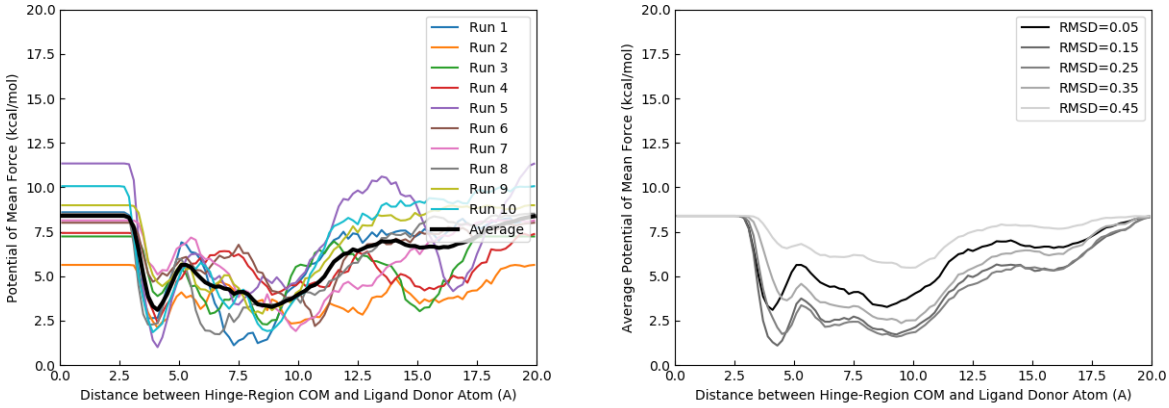

Figure S6.3. (a) JAK-200 structure (b) PMF curve of JH2-JAK200 unbinding at 0.05 Å Val629 backbone RMSD (c) PMF curves of JH2/JAK-200 unbinding at highly-sampled Val629 backbone RMSDs. All PMF curves converged from 0 until at least 10 angstroms.

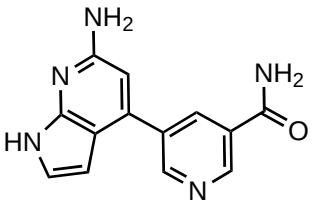

JAK-201

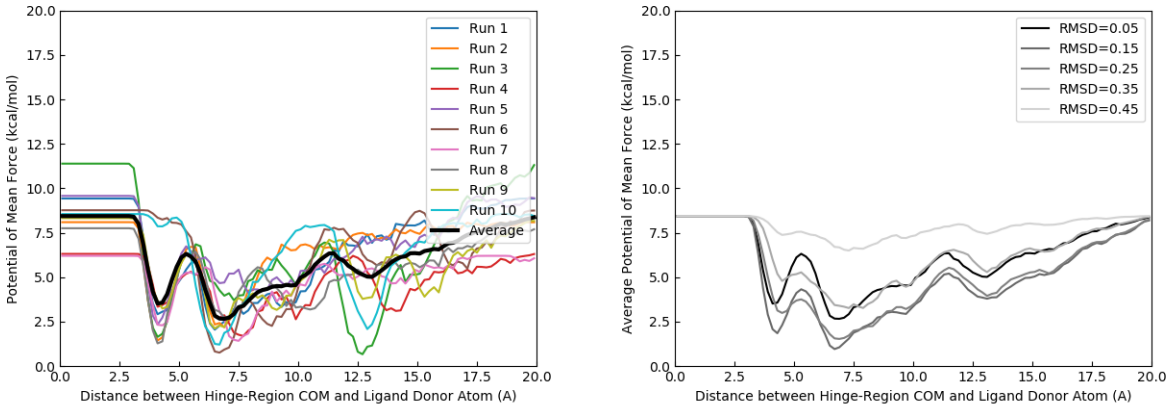

Figure S6.4. (a) JAK-201 structure (b) PMF curve of JH2/JAK-201 unbinding at 0.05 Å Val629 backbone RMSD (c) PMF curves of JH2/JAK-201 unbinding at highly-sampled Val629 backbone RMSDs. All PMF curves converged from 0 until at least 10 angstroms.

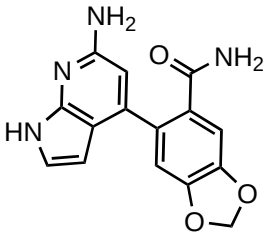

JAK-202

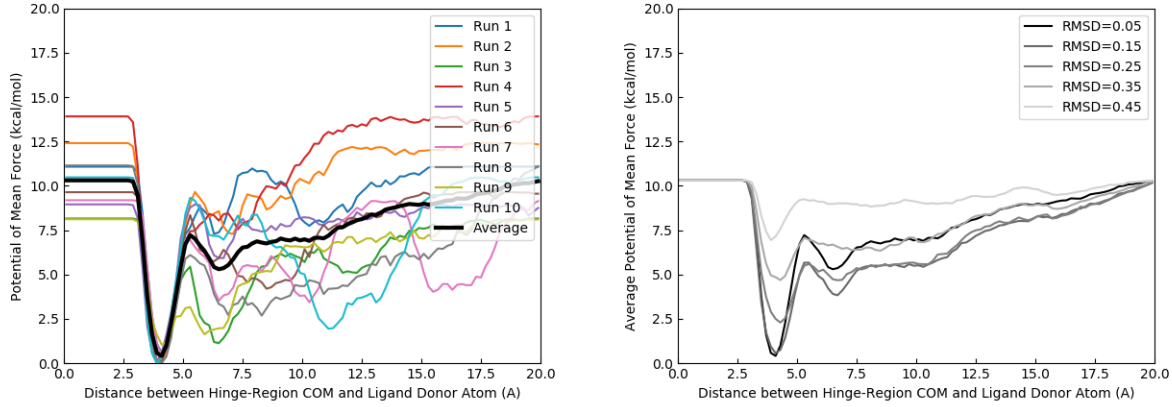

Figure S6.5. (a) JAK-202 structure (b) PMF curve of JH2/JAK-202 unbinding at 0.05 Å Val629 backbone RMSD (c) PMF curves of JH2/JAK-202 unbinding at highly-sampled Val629 backbone RMSDs. All PMF curves converged from 0 until at least 10 angstroms.

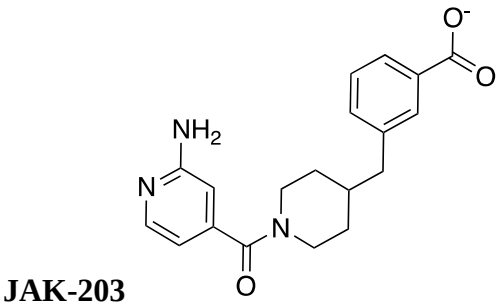

JAK-203

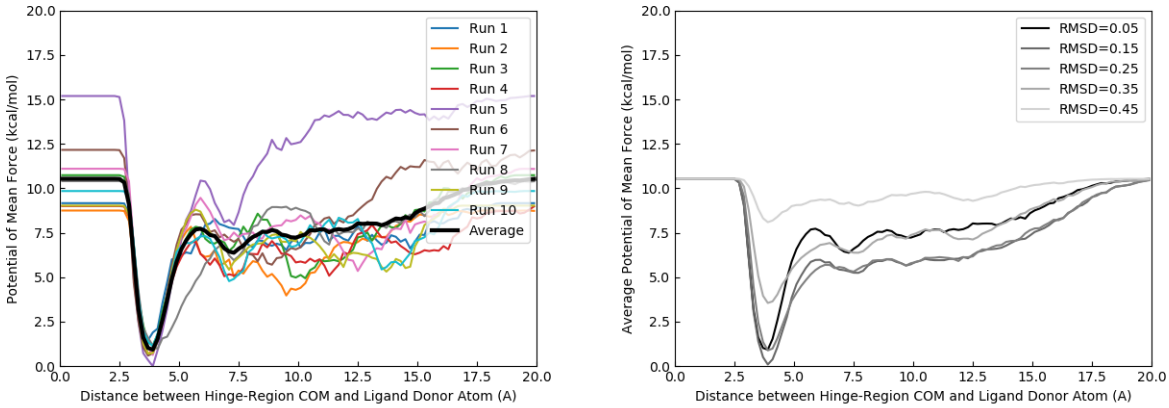

Figure S6.6. (a) JAK-203 structure (b) PMF curve of JH2/JAK-203 unbinding at 0.05 Å Val629 backbone RMSD (c) PMF curves of JH2/JAK-203 unbinding at highly-sampled Val629 backbone RMSDs. All PMF curves converged from 0 until at least 10 angstroms.

JAK-204

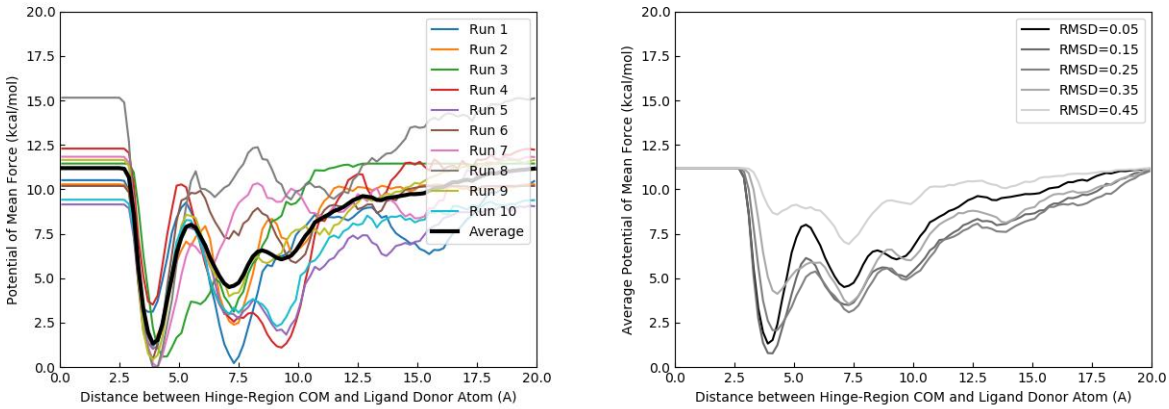

Figure S6.7. (a) JAK-204 structure (b) PMF curve of JH2/JAK-204 unbinding at 0.05 Å Val629 backbone RMSD (c) PMF curves of JH2/JAK-204 unbinding at highly-sampled Val629 backbone RMSDs. All PMF curves converged from 0 until at least 10 angstroms.

JAK-205

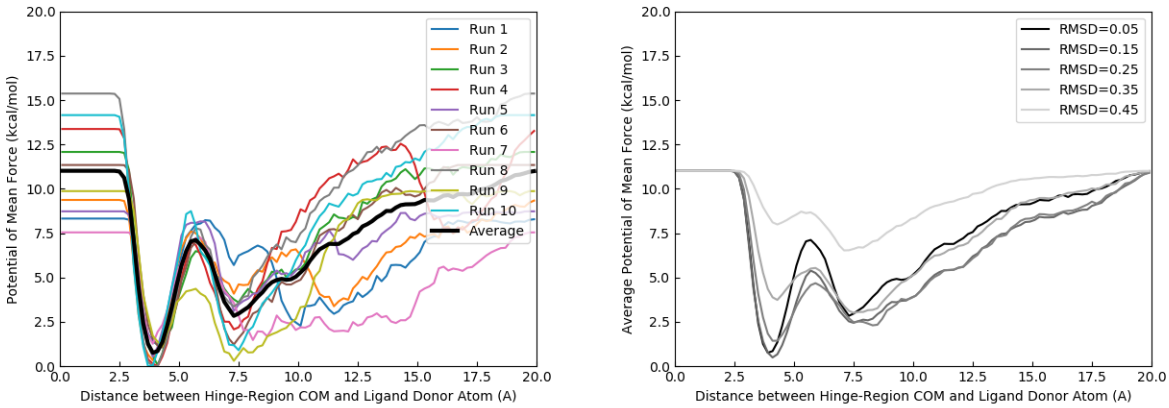

Figure S6.8. (a) JAK-205 structure (b) PMF curve of JH2/JAK-205 unbinding at 0.05 Å Val629 backbone RMSD (c) PMF curves of JH2/JAK-205 unbinding at highly-sampled Val629 backbone RMSDs. All PMF curves converged from 0 until at least 10 angstroms.

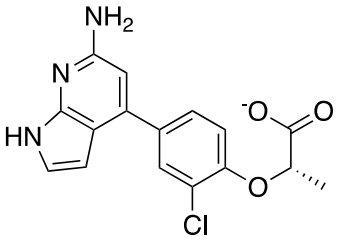

JAK-206

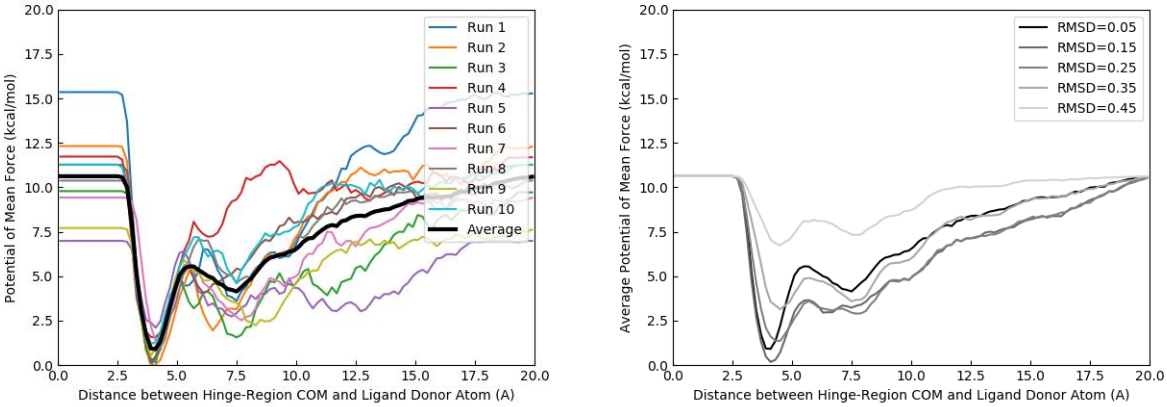

Figure S6.9. (a) JAK-206 structure (b) PMF curve of JH2/JAK-206 unbinding at 0.05 Å Val629 backbone RMSD (c) PMF curves of JH2/JAK-206 unbinding at highly-sampled Val629 backbone RMSDs. All PMF curves converged from 0 until at least 10 angstroms.

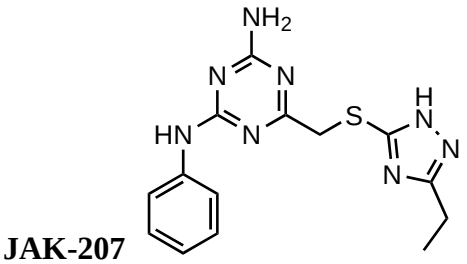

JAK-207

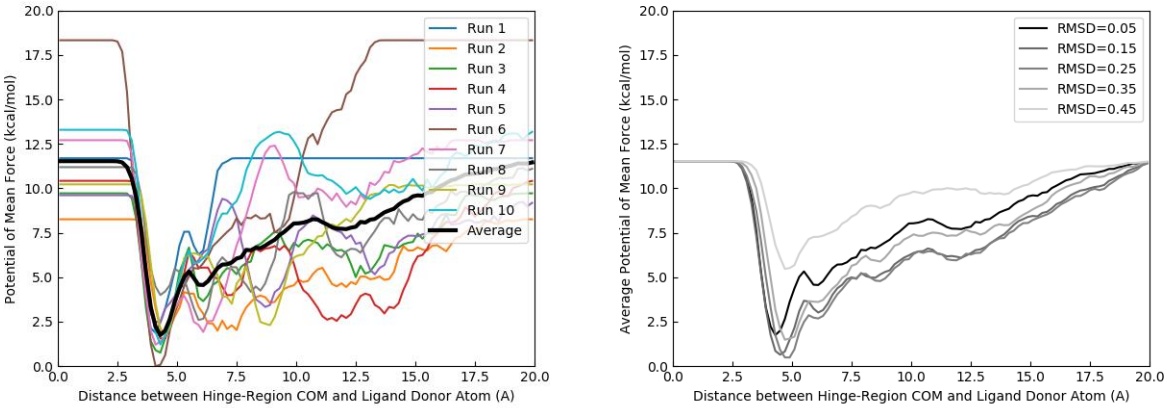

Figure S6.10. (a) JAK-207 structure (b) PMF curve of JH2/JAK-207 unbinding at 0.05 Å Val629 backbone RMSD (c) PMF curves of JH2/JAK-207 unbinding at highly-sampled Val629 backbone RMSDs. All PMF curves converged from 0 until at least 10 angstroms. Run 1 was excluded in the PMF curve average because there was not enough sampling at 0.05 Å Val629 backbone RMSD.

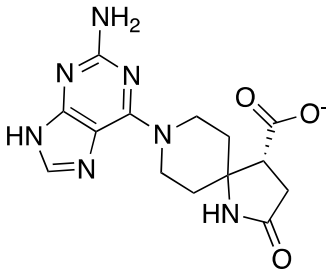

JAK-208

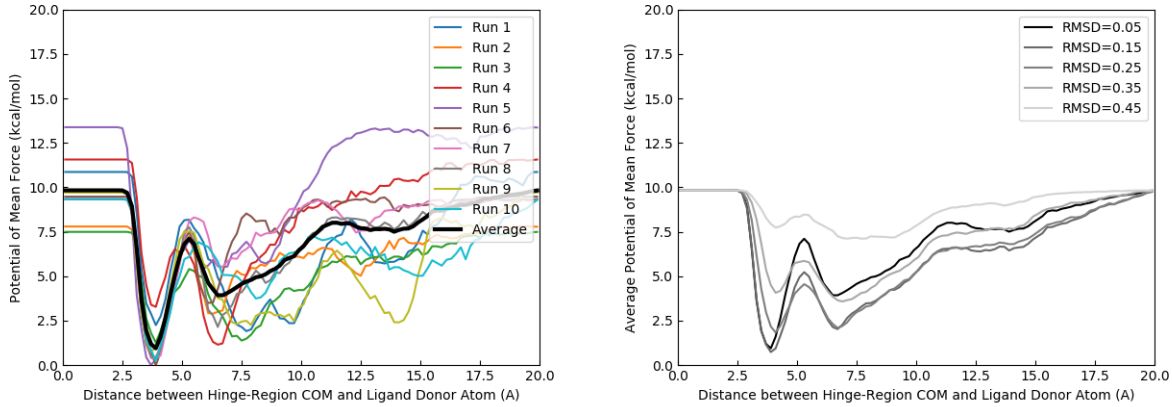

Figure S6.11. (a) JAK-208 structure (b) PMF curve of JH2/JAK-208 unbinding at 0.05 Å Val629 backbone RMSD (c) PMF curves of JH2/JAK-208 unbinding at highly-sampled Val629 backbone RMSDs. All PMF curves converged from 0 until at least 10 angstroms.

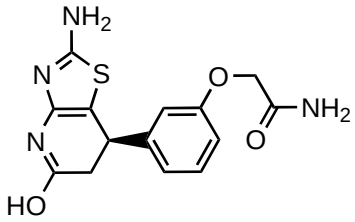

JAK-209

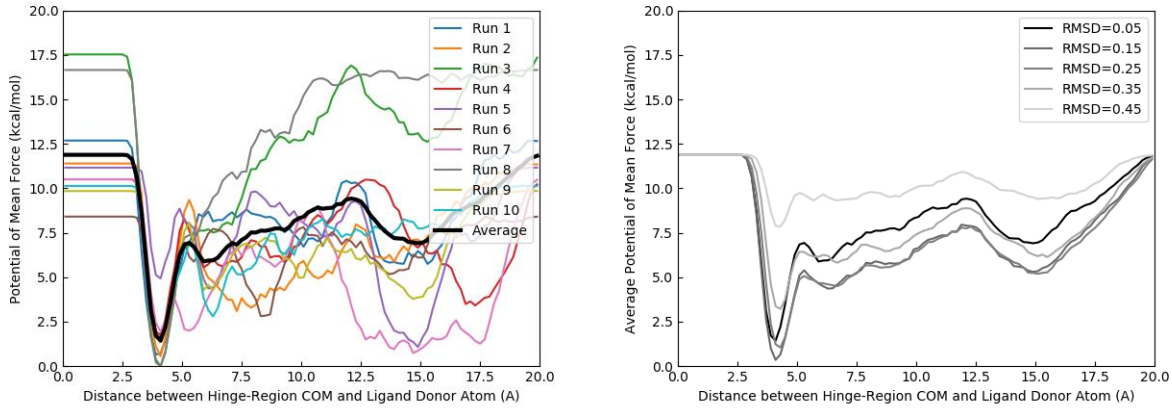

Figure S6.12. (a) JAK-209 structure (b) PMF curve of JH2/JAK-209 unbinding at 0.05 Å Val629 backbone RMSD (c) PMF curves of JH2/JAK-209 unbinding at highly-sampled Val629 backbone RMSDs. All PMF curves converged from 0 until at least 10 angstroms.

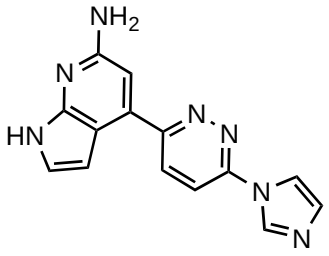

JAK-210

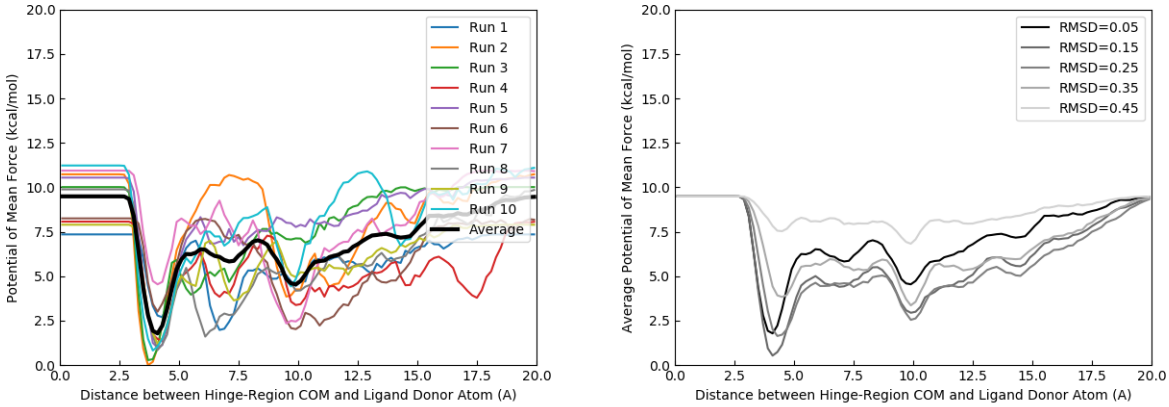

Figure S6.13. (a) JAK-210 structure (b) PMF curve of JH2/JAK-210 unbinding at 0.05 Å Val629 backbone RMSD (c) PMF curves of JH2/JAK-210 unbinding at highly-sampled Val629 backbone RMSDs. All PMF curves converged from 0 until at least 10 angstroms.

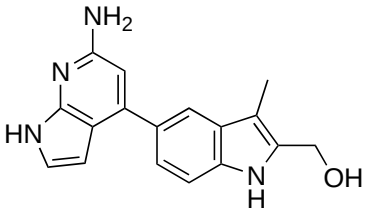

JAK-211

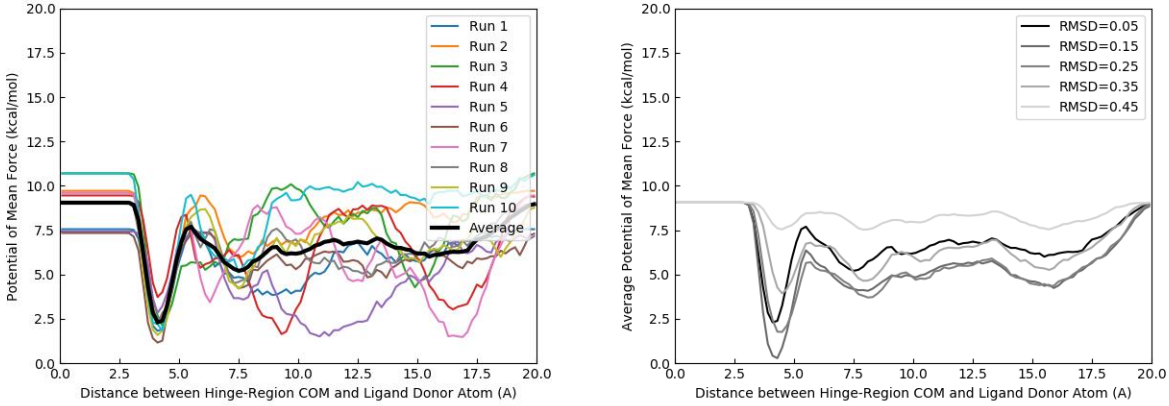

Figure S6.14. (a) JAK-211 structure (b) PMF curve of JH2/JAK-211 unbinding at 0.05 Å Val629 backbone RMSD (c) PMF curves of JH2/JAK-211 unbinding at highly-sampled Val629 backbone RMSDs. All PMF curves converged from 0 until at least 10 angstroms.

JAK-212

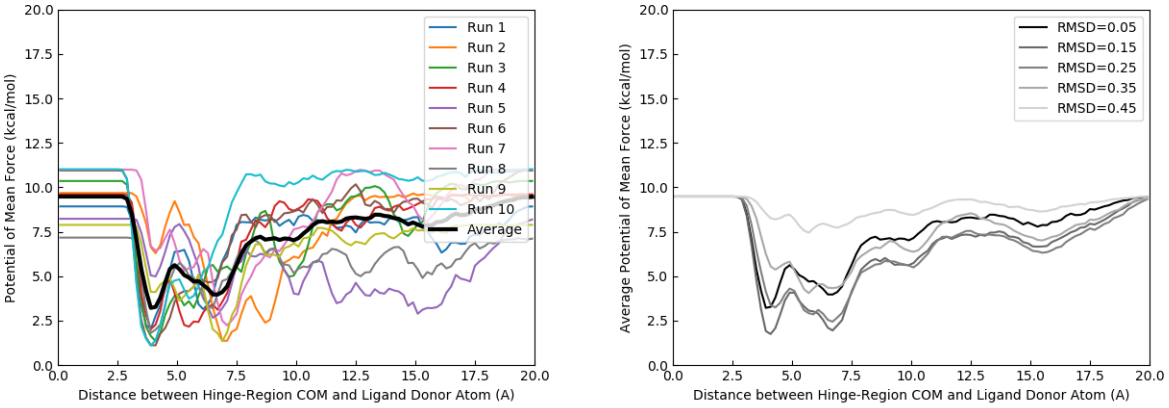

Figure S6.15. (a) JAK-212 structure (b) PMF curve of JH2/JAK-212 unbinding at 0.05 Å Val629 backbone RMSD (c) PMF curves of JH2/JAK-212 unbinding at highly-sampled Val629 backbone RMSDs. All PMF curves converged from 0 until at least 10 angstroms.

JAK-213

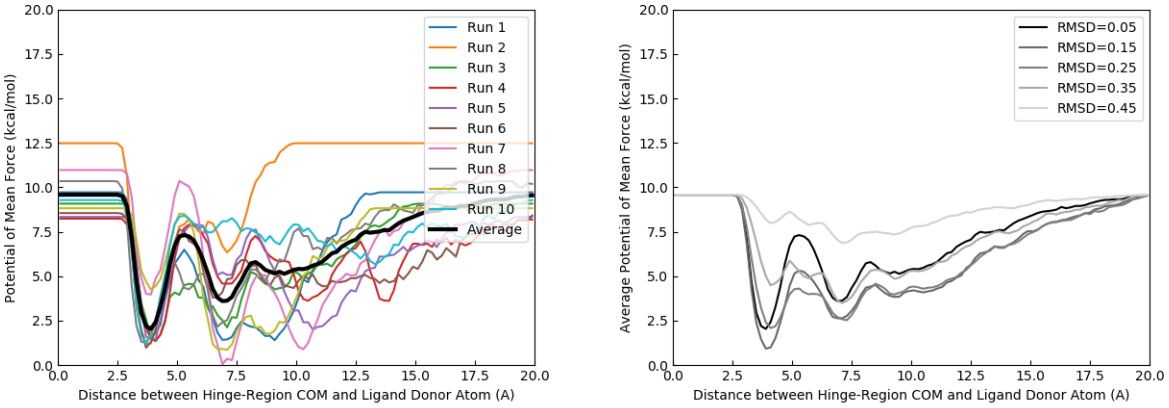

Figure S6.16. (a) JAK-213 structure (b) PMF curve of JH2/JAK-213 unbinding at 0.05 Å Val629 backbone RMSD (c) PMF curves of JH2/JAK-213 unbinding at highly-sampled Val629 backbone RMSDs. All PMF curves converged from 0 until at least 10 angstroms.

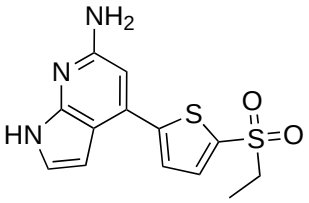

JAK-214

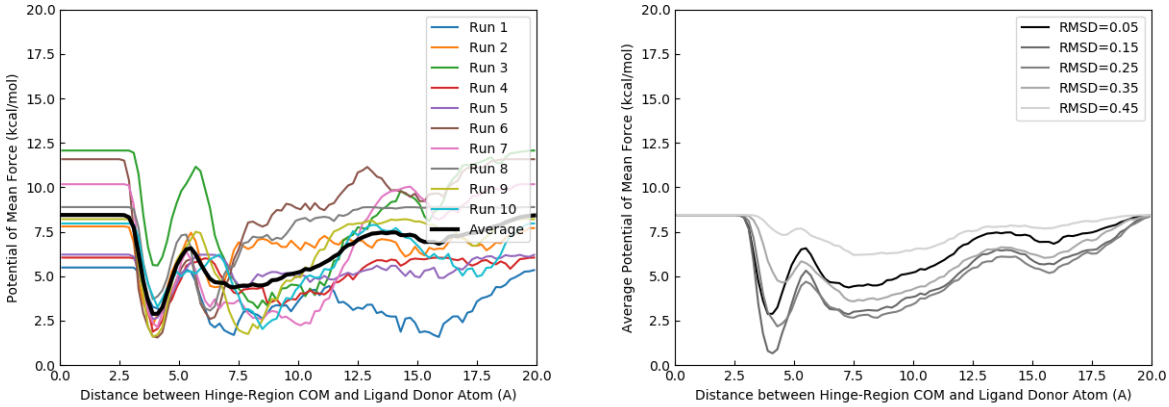

Figure S6.17. (a) JAK-214 structure (b) PMF curve of JH2/JAK-214 unbinding at 0.05 Å Val629 backbone RMSD (c) PMF curves of JH2/JAK-214 unbinding at highly-sampled Val629 backbone RMSDs. All PMF curves converged from 0 until at least 10 angstroms.

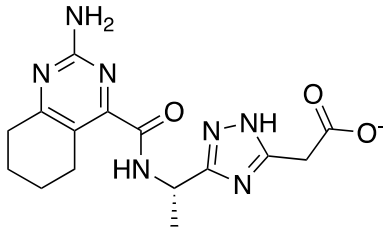

JAK-215

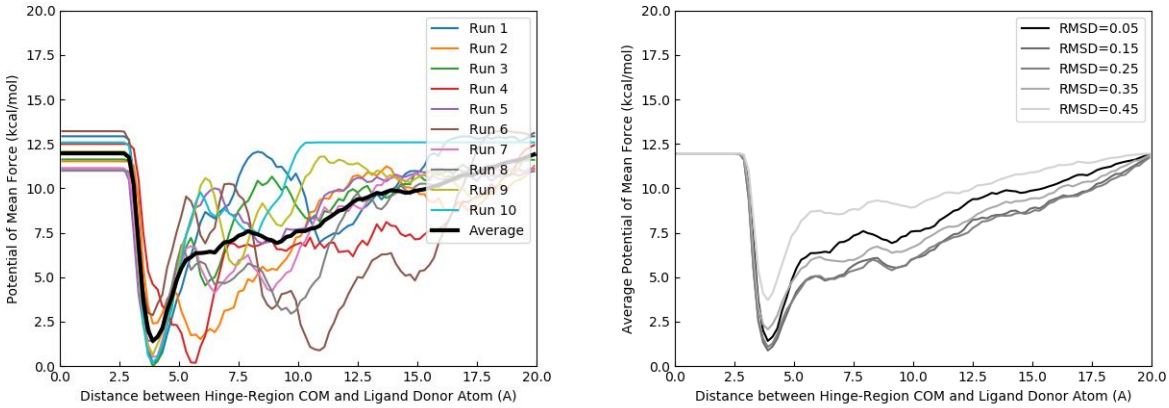

Figure S6.18. (a) JAK-215 structure (b) PMF curve of JH2/JAK-215 unbinding at 0.05 Å Val629 backbone RMSD (c) PMF curves of JH2/JAK-215 unbinding at highly-sampled Val629 backbone RMSDs. All PMF curves converged from 0 until at least 10 angstroms.

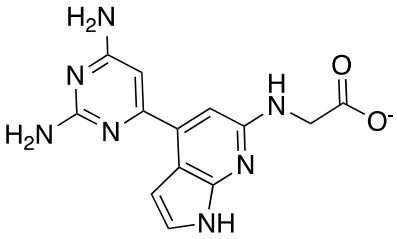

JAK-216

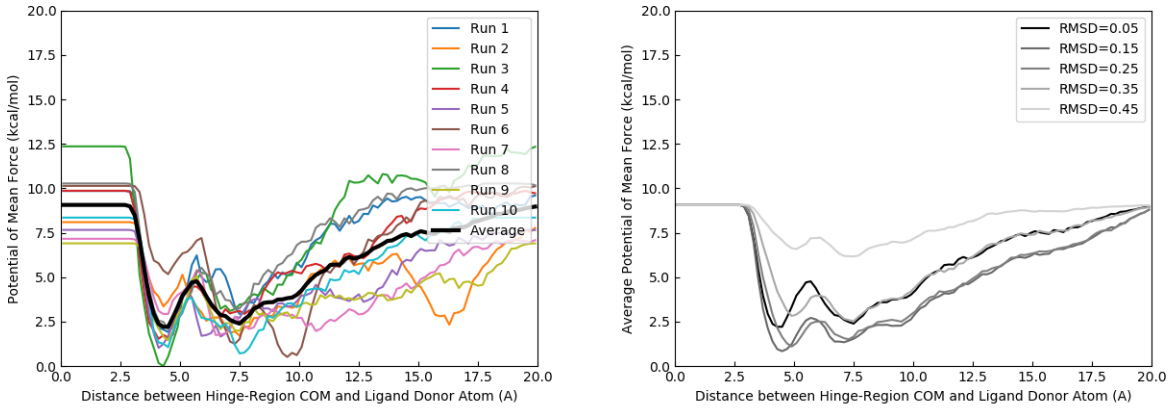

Figure S6.19. (a) JAK-216 structure (b) PMF curve of JH2/JAK-216 unbinding at 0.05 Å Val629 backbone RMSD (c) PMF curves of JH2/JAK-216 unbinding at highly-sampled Val629 backbone RMSDs. All PMF curves converged from 0 until at least 10 angstroms.

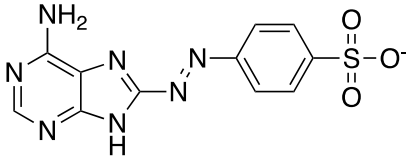

JAK-217

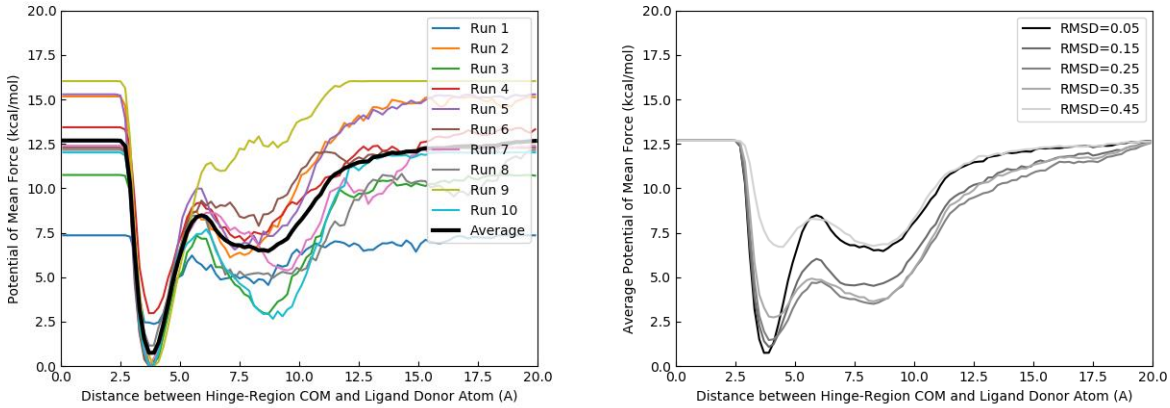

Figure S6.20. (a) JAK-217 structure (b) PMF curve of JH2/JAK-217 unbinding at 0.05 Å Val629 backbone RMSD (c) PMF curves of JH2/JAK-217 unbinding at highly-sampled Val629 backbone RMSDs. All PMF curves converged from 0 until at least 10 angstroms.

JAK-218

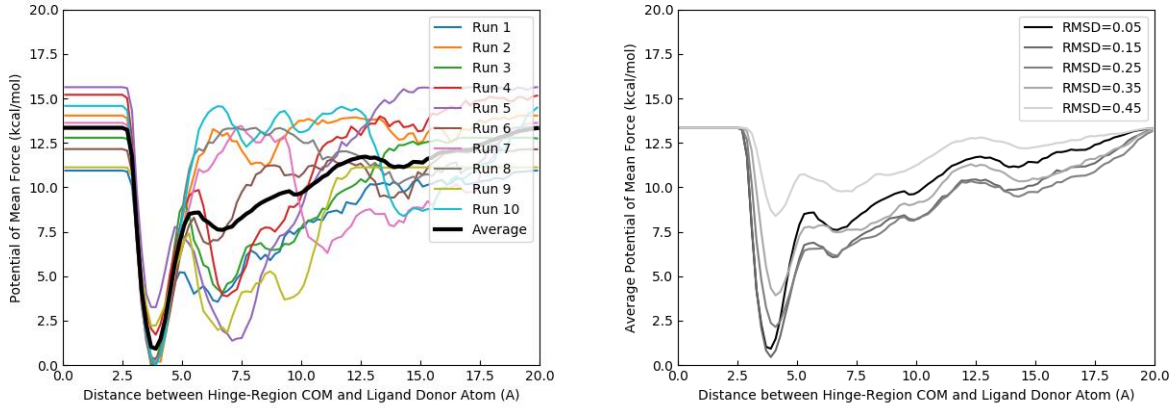

Figure S6.21. (a) JAK-218 structure (b) PMF curve of JH2/JAK-218 unbinding at 0.05 Å Val629 backbone RMSD (c) PMF curves of JH2/JAK-218 unbinding at highly-sampled Val629 backbone RMSDs. All PMF curves converged from 0 until at least 10 angstroms.

JAK-219

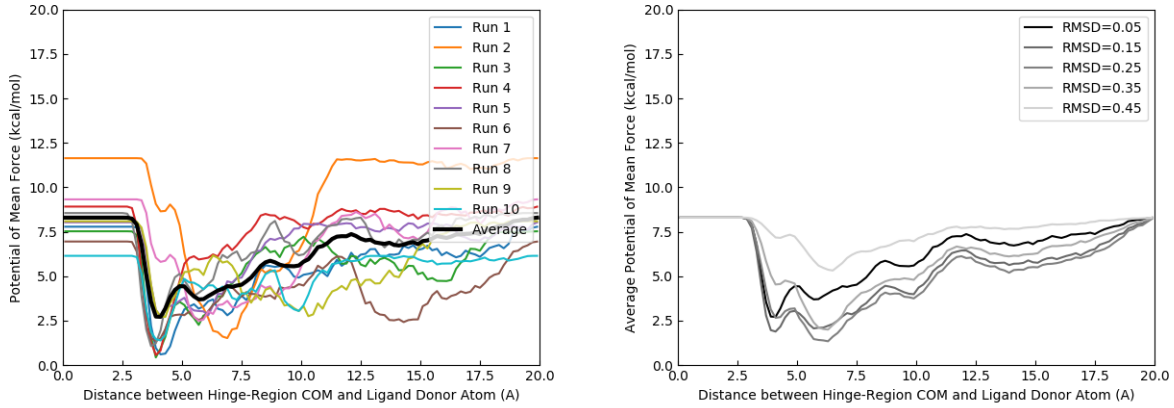

Figure S6.22. (a) JAK-219 structure (b) PMF curve of JH2/JAK-219 unbinding at 0.05 Å Val629 backbone RMSD (c) PMF curves of JH2/JAK-219 unbinding at highly-sampled Val629 backbone RMSDs. All PMF curves converged from 0 until at least 10 angstroms.

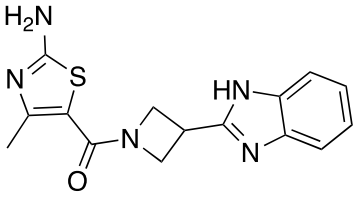

JAK-220

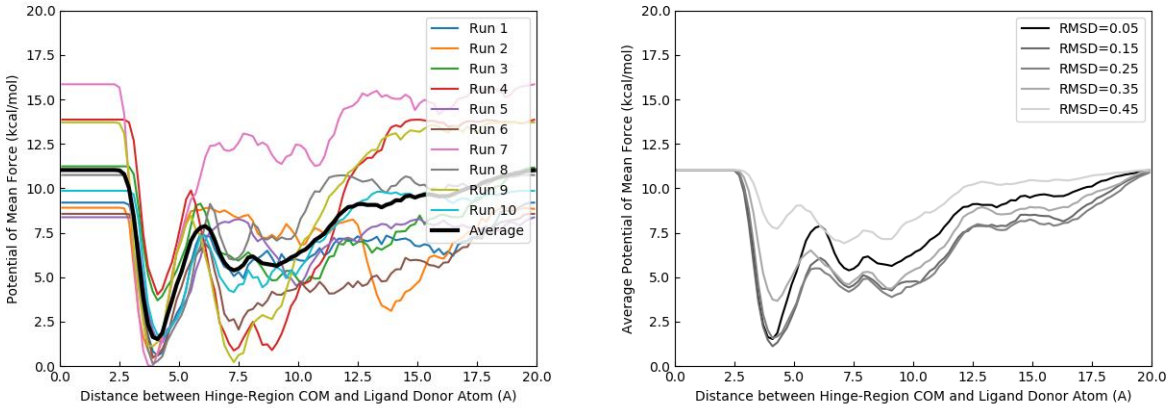

Figure S6.23. (a) JAK-220 Structure (b) PMF curve of JH2/JAK-220 unbinding at 0.05 Å Val629 backbone RMSD (c) PMF curves of JH2/JAK-220 unbinding at highly-sampled Val629 backbone RMSDs. All PMF curves converged from 0 until at least 10 angstroms.

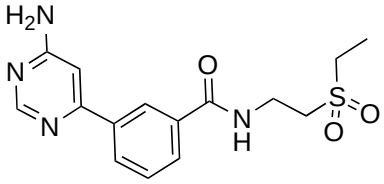

JAK-221

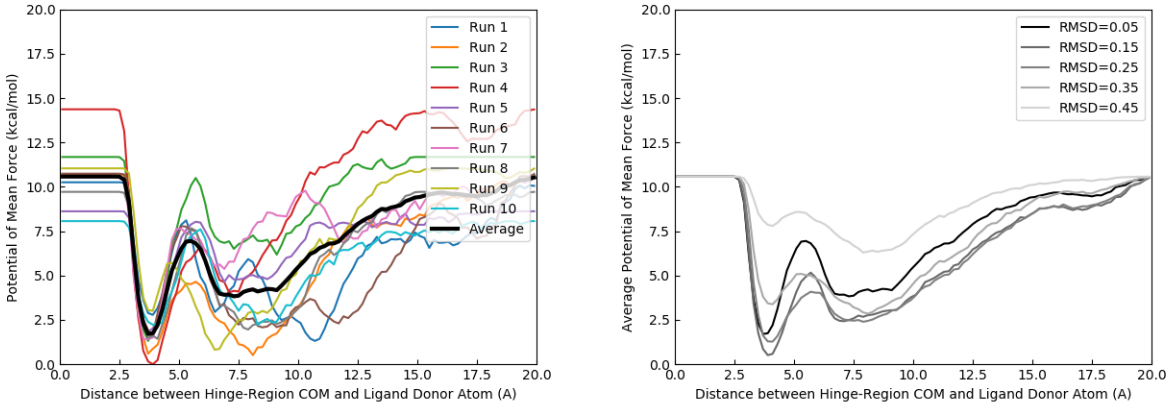

Figure S6.24. (a) JAK-221 structure (b) PMF curve of JH2/JAK-221 unbinding at 0.05 Å Val629 backbone RMSD (c) PMF curves of JH2/JAK-221 unbinding at highly-sampled Val629 backbone RMSDs. All PMF curves converged from 0 until at least 10 angstroms.

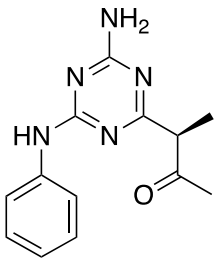

JAK-222

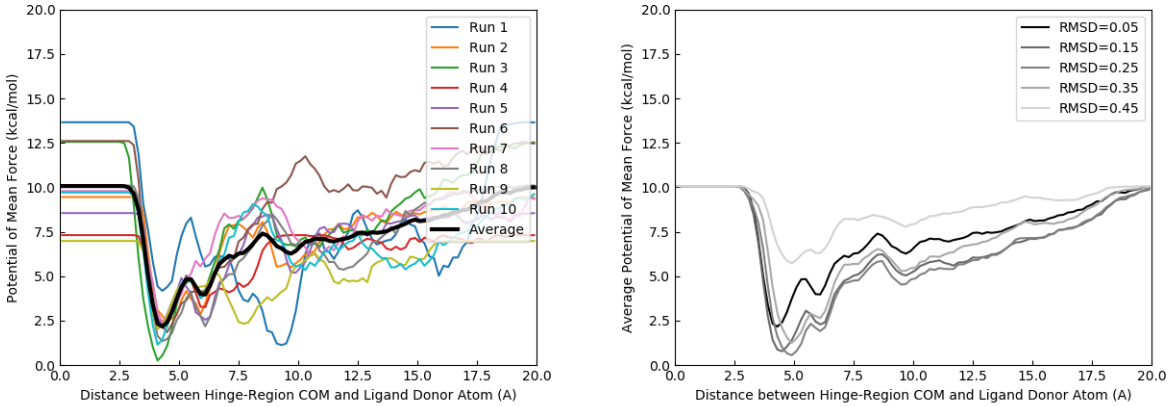

Figure S6.25. (a) JAK-222 structure (b) PMF curve of JH2/JAK-222 unbinding at 0.05 Å Val629 backbone RMSD (c) PMF curves of JH2/JAK-222 unbinding at highly-sampled Val629 backbone RMSDs. All PMF curves converged from 0 until at least 10 angstroms.

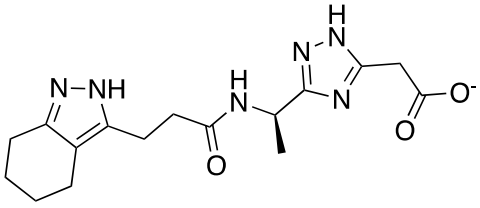

JAK-223

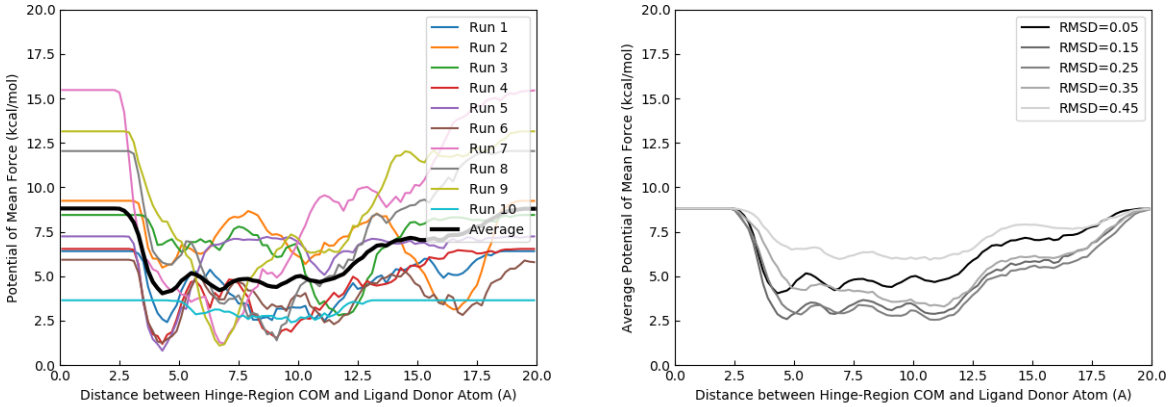

Figure S6.26. (a) JAK-223 structure (b) PMF curve of JH2/JAK-223 unbinding at 0.05 Å Val629 backbone RMSD (c) PMF curves of JH2/JAK-223 unbinding at highly-sampled Val629 backbone RMSDs. All PMF curves converged from 0 until at least 10 angstroms.

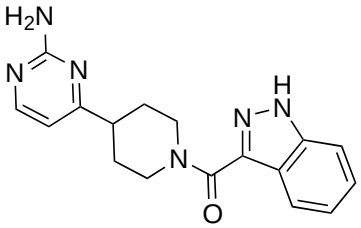

JAK-224

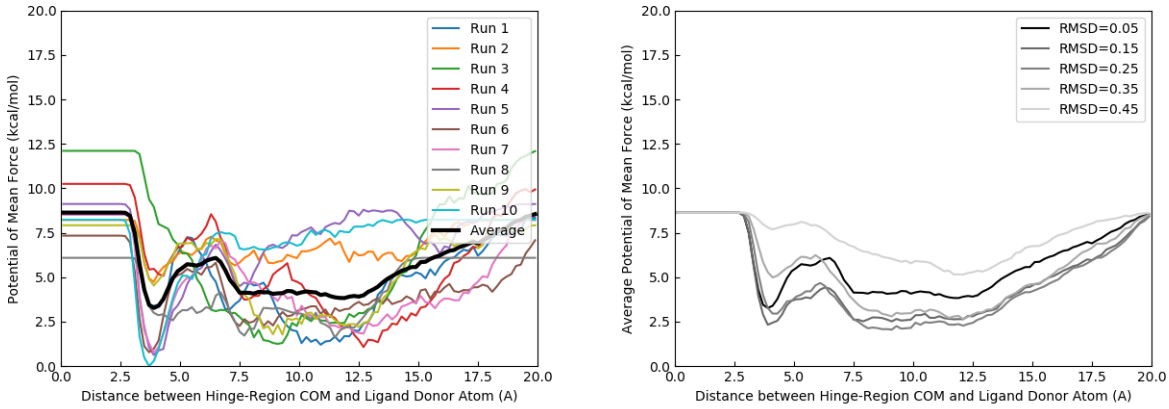

Figure S6.27. (a) JAK-224 structure (b) PMF curve of JH2/JAK-224 unbinding at 0.05 Å Val629 backbone RMSD (c) PMF curves of JH2/JAK-224 unbinding at highly-sampled Val629 backbone RMSDs. All PMF curves converged from 0 until at least 10 angstroms.

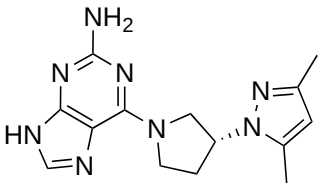

JAK-225

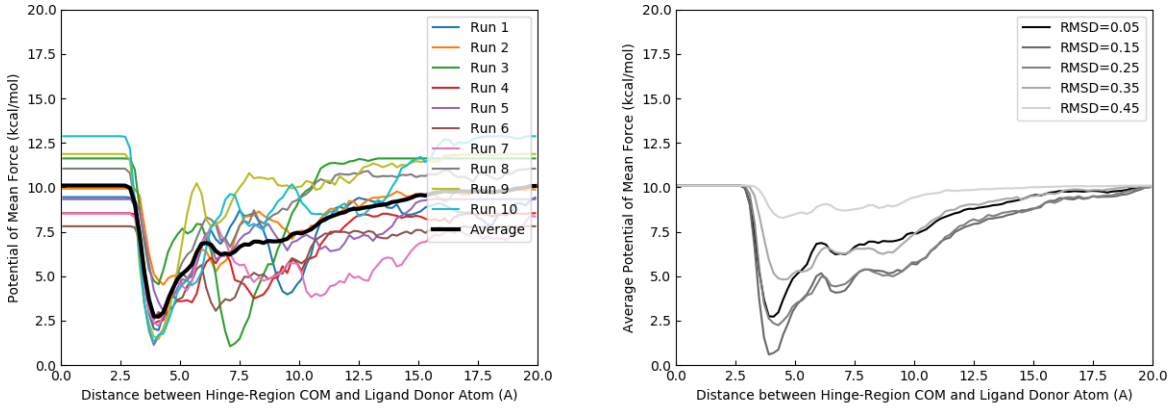

Figure S6.28. (a) JAK-225 structure (b) PMF curve of JH2/JAK-225 unbinding at 0.05 Å Val629 backbone RMSD (c) PMF curves of JH2/JAK-225 unbinding at highly-sampled Val629 backbone RMSDs. All PMF curves converged from 0 until at least 10 angstroms.

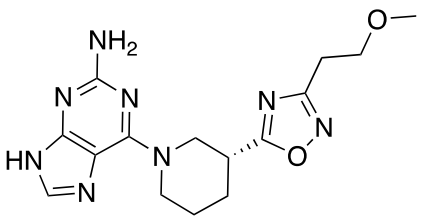

JAK-226

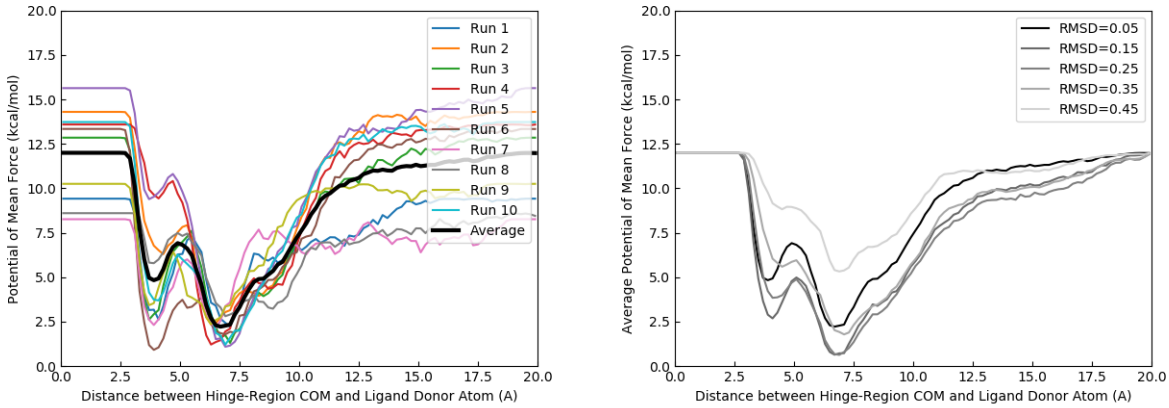

Figure S6.29. (a) JAK-226 structure (b) PMF curve of JH2/JAK-226 unbinding at 0.05 Å Val629 backbone RMSD (c) PMF curves of JH2/JAK-226 unbinding at highly-sampled Val629 backbone RMSDs. All PMF curves converged from 0 until at least 10 angstroms

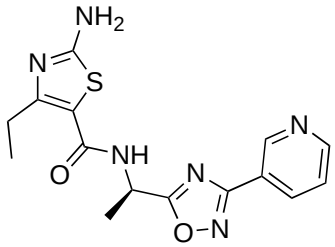

JAK-227

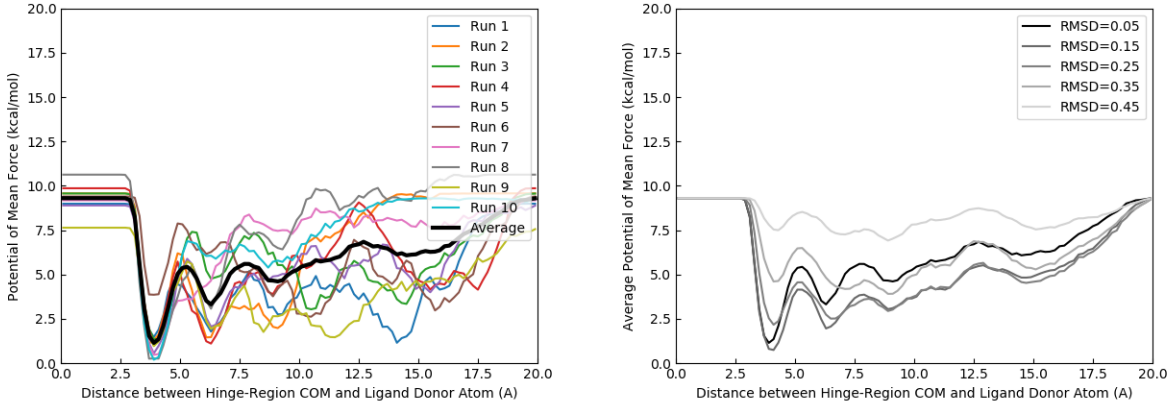

Figure S6.30. (a) JAK-227 structure (b) PMF curve of JH2/JAK-227 unbinding at 0.05 Å Val629 backbone RMSD (c) PMF curves of JH2/JAK-227 unbinding at highly-sampled Val629 backbone RMSDs. All PMF curves converged from 0 until at least 10 angstroms**.**